

5 **Exploring the 4D scales of Using repeat UAV based laser scanning and multispectral imagery to explore eco-geomorphic interactions/feedbacks along a river corridor using repeat UAV Laser Scanning (UAV-LS), multispectral imagery, and a functional traits framework.**

Christopher Tomsett¹, Julian Leyland¹

¹School of Geography and Environmental Science, University of Southampton, Highfield, Southampton, SO17 1BJ, UK.

Correspondence to: Christopher Tomsett (C.G.Tomsett@soton.ac.uk)

10 **Abstract.** Vegetation plays a critical role in the modulation of fluvial process and morphological evolution. However, adequately capturing the spatial and temporal variability and complexity of vegetation characteristics remains a challenge. Currently, most of the research seeking to address these issues takes place at either the individual plant scale or via larger scale bulk roughness classifications, with the former typically seeking to characterise vegetation-flow interactions and the latter identifying spatial variation in vegetation types. Herein, we devise a method which extracts functional vegetation traits using
15 UAV laser scanning and multispectral imagery, and upscale these to reach scale functional group classifications. Simultaneous monitoring of morphological change is undertaken to identify eco-geomorphic links between different functional groups and the geomorphic response of the system. Identification of four groups from quantitative structural modelling and two further groups from image analysis was achieved and were upscaled to reach-scale group classifications with an overall accuracy of 80%. ~~Plant structure was then used to assess seasonal changes in excess vegetative drag~~For each functional group, the
20 directions and relate these to magnitudes of geomorphic change across the study site were assessed over four time periods, comprising of two summers and winters. This research reveals that remote sensing offers a possible solution to the difficulty of challenges in scaling traits-based approaches for eco-geomorphic research, and that future work should investigate how these methods may be applied to different functional groups and to larger areas using airborne laser scanning and satellite imagery datasets.

25 **1. Introduction**

Fluvial eco-geomorphic interactions are co-dependent, complex, and variable across space and time, representing a continued area of interest within river research (Thoms and Parsons, 2002). The diversity of eco-geomorphology in river corridors can be attributed to surrounding land use, existing morphology, and flood regimes (Naiman et al., 1993), whilst this same diversity simultaneously influences the flow of water and sediment, ultimately affecting morphology (Diehl et al., 2017a) and floodplain
30 conveyance (Nepf and Vivoni, 2000). The role of vegetation within the river corridor is well established, benefiting the local

ecology (Harvey and Gooseff, 2015; Sweeney et al., 2004) alongside playing a role in natural flood management schemes and reconnecting channels and floodplains (Lane, 2017; Wilkinson et al., 2019), ~~especially for small catchments where land cover is more influential for flooding (Blöschl et al., 2007).~~ This is important when considered against a backdrop of a rapidly changing climate where flow extremes are more varied, flooding more likely (Unisdr and Cred, 2015)(Unisdr and Cred, 2015), and riparian vegetation is likely to undergo shifts in composition (Rivaes et al., 2014; Palmer et al., 2009). Consequently, adequately measuring and monitoring vegetation ~~with~~within the fluvial domain is critical to understanding how these systems will respond to varying climatic and ~~hydrological~~hydraulic conditions.

The characterisation of riparian vegetation distribution over larger (>1 km) scales has typically relied upon the use of coarse classifications such as those identified in the Water Framework Directive (e.g. Gilvear et al., 2004), using techniques such as aerial imagery and satellite remote sensing (see Tomsett and Leyland, 2019). ~~Any~~Advances in higher resolution techniques, in particular mobile laser scanning, have enabled the possibility to capture vegetation data in enough detail to establish individual plant structure (e.g. Brede et al., 2019; Hyyppä et al., 2020; Liang et al., 2014). Yet any characterisation must be scalable and geographically transferable to cover the vast range of different fluvial landscapes, whilst still accounting for the complexity presented within individual river corridors. Over-simplified, coarse classifications may altogether miss the ~~vegetation~~ complexity that exists, whilst conversely, highly detailed models tend to be necessarily localised and less transferable to alternate systems ~~and scenarios.~~

Traits-based classifications, developed and used within ecology, offer a scalable and transferable approach which can be applicable to the fluvial domain (Diehl et al., 2017a), and have been shown to be useful for modelling topographic response to changing vegetation, sediment, and flow conditions (Diehl et al., 2018; Butterfield et al., 2020). However, the application of traits-based classifications over larger reaches has yet to be fully realised, due to the challenges in collecting appropriately high resolution data at these scales (e.g. >1 km). If such challenges can be overcome, it offers an opportunity for those analysing vegetation both within the river corridor and elsewhere in the landscape to obtain spatially explicit data on vegetation that was previously unattainable.

To address these gaps, ~~herein we examine the scales over which different traits can be collected from~~ ~~utilise~~ remote sensing methods ~~to collect data from which vegetation traits are extracted~~ and assess how well these ~~traits~~ can be used to establish eco-geomorphic relationships. We use a UK based temperate river as an example site to demonstrate the effectiveness of novel remote sensing techniques for characterising vegetation. ~~We investigate, investigating~~ the limits of trait detection and the scales at which they are most appropriately used to enhance eco-geomorphic understanding, ~~enabling us to establish the applicability of these methods to a variety of river corridor environments. Below we introduce the concepts of plant functional traits and hydraulically relevant traits before establishing the aims of this research.~~

1.1. The Importance of Vegetation

65 It is well understood that vegetation plays a key role within the river corridor and that how vegetation is represented in models
(e.g. constant and varying roughness values, rigid cylinders etc.) can affect the outcomes of hydrodynamic simulations.
Channels with in-stream vegetation may experience roughness values an order of magnitude higher than non-vegetated
channels (De Doncker et al., 2009), capable of reducing velocities by up to 90% (Sand-Jensen and Pedersen, 1999), with stem
shape, ~~the amount of foliage,~~ and deformation ~~at various flow stages,~~ all influencing ~~river~~ flow (James et al., 2008). The
70 challenges posed by quantifying in-stream vegetation means that it is often difficult to make estimations of in-stream roughness
(~~O'hare et al., 2014~~)(~~O'hare et al., 2011~~). Conversely, terrestrial vegetation that influences flow during periods of flooding is
easier to measure and monitor depending on the scales of analysis. ~~Banks are typically eroded via mechanisms of mass failures
or entrainment (Hughes, 2016) and so any stabilising effects of vegetation must influence these processes.~~ Vegetation can
reduce stream power, increase soil cohesion, and influence soil moisture levels, all of which can help to ~~reduce~~limit bank
75 erosion (Simon et al., 2000; Fox et al., 2007; Kang, 2012). Bank collapse is influenced by three dominant factors, the extra
mass of the vegetation, the shear strength provided by root reinforcement, and changes to bank pore water pressure (Wiel and
Darby, 2007), with above ground biomass therefore directly influencing the mechanical and hydraulic properties of the
substrate (Gurnell, 2014). The above ground biomass also has a direct influence on river flow and sediment transport when
submerged (Gurnell, 2014), acting as a sediment trap and stabilising bars (Hortobágyi et al., 2018; Sharpe and James, 2006),
80 although this is stage dependent and ~~depends on plant volume and structure~~varies with plant volume and structure. Therefore
being adequately able to capture such data over reach scales is critical for understanding the feedback loops between vegetation,
flow, and morphology.

~~The below ground biomass is of equal importance, with root networks decreasing the erodibility of beds and banks by
85 increasing the critical shear stress required for erosion to take place (Millar and Quick, 1998; Wiel and Darby, 2007). The
presence of grass compared to bare sediment can increase the stability of soil by a factor of 1.97 (Julian and Torres, 2006) and
that comparing trees to grass can lead to similar increases in stability (Millar and Quick, 1998; Huang and Nanson, 1998).
Furthermore, the below ground portion of vegetation is highly influential in vegetation removal during peak flow events
(Caponi et al., 2020; Bankhead et al., 2017; Francalanci et al., 2020), a critical phase in the feedback loops between vegetation,
90 flow, and morphology. Yet the difficulties in obtaining below ground data is well noted when compared to above ground data,
and continues to remain a challenge for remote sensing studies.~~

1.2. Plant Functional Traits

A functional traits-based approach offers a way to represent vegetation data at reach scale and beyond. Functional traits
originate from ecological research, and are morphological, physiological, and phenological attributes that can be measured at
95 the individual plant level (Violle et al., 2007; Kattge et al., 2011; Savage et al., 2007).~~These can either be direct measurements~~

of a function, such as photosynthesis, or a surrogate measure for that function, such as leaf area, but to be classed as functional in ecology these must either affect plant growth, reproduction or survival (Violle et al., 2007; Quétier et al., 2007). These measured traits can either be an effect or response trait, whereby they either have an influence on or are influenced by their surrounding environment respectively (Violle et al., 2007; Kattge et al., 2020).

100 One of the benefits of collecting traits-based data, is the ability to group plants that display similar functional traits into functional groups (Blondel, 2003). This provides a scalable framework for eco-geomorphic research, increasing the applicability of research at one site to another without the need for the same species, but only the need for those species to have similar traits (Megill et al., 2006). Therefore, the findings of a community response to factors such as land use change or
105 climate change in one location can be applied to different locations with similar trait compositions (De Bello et al., 2006; Garnier et al., 2006). This is supported in findings by Tabacchi et al. (2019) into bio-geomorphological succession, whereby taxonomic approaches worked well but traits based methods accounted for variation in local and regional conditions better, which is essential for scalability. Herein we specifically use the term 'functional group' (*sensu* Blondel, 2003) because we explore how aggregated ecosystem processes ultimately affect geomorphological response. This approach allows for increased
110 applicability to different reaches that contain similar functional groups (Mcgill et al., 2006; De Bello et al., 2006; Garnier et al., 2006), and accounts for variation in local and regional conditions better than purely taxonomic approaches (Tabacchi et al., 2019).

Traits-based approaches are well suited for eco-geomorphic research due to the strong environmental gradients within fluvial systems (Naiman et al., 2005). ~~Vegetation responds to hydrological variables, such as water availability and disturbance events (Hupp and Osterkamp, 1996)~~ Vegetation responds to hydrological variables, such as water availability and disturbance events (Hupp and Osterkamp, 1996) whilst also influencing flow, sediment transport, and morphological stability (Gurnell, 2014), meaning that the bi-directional nature of this relationship maps well onto a traits-based framework. ~~O'hare et al. (2016) have assessed the traits of nearly 500 species that influence river processes, revealing evidence of a broad link between plant form, distribution, and~~ Both plant form and distribution have been linked to stream power within the UK (O'hare et al., 2014). Moreover, traits based approaches allow for a more comprehensive view on eco-geomorphic interactions than a purely taxonomic approach due to the environmental conditions having a larger influence on trait compositions than species compositions (O'hare et al., 2011), with fluvial conditions also being shown to have a greater influence on trait composition than species composition (Göthe et al., 2017; Corenblit et al., 2015).

125 To date, ~~the majority of most~~ traits-based research has focussed on ecological responses to environmental conditions. For example, greater inundation likelihood has been shown to increase the presence of plants with longer and younger leaves (Stromberg and Merritt, 2016; Meeoy-Sulentie et al., 2017) whilst also being less woody (Kyle and Leishman, 2009; Stromberg and Merritt, 2016). ~~Conversely, which are less woody, whereas~~ plants in lower stress environments tend to be taller with longer

130 life cycles (Kyle and Leishman, 2009; Stromberg and Merritt, 2016; McCoy-Sulentic et al., 2017). ~~Factors such as nutrient loading (Baattrup Pedersen et al., 2016; Lukacs et al., 2019), light conditions (Baattrup Pedersen et al., 2015), carbon availability (Lukacs et al., 2019), and anthropogenic interference (Baattrup Pedersen et al., 2002; O'briain et al., 2017) are all key controllers of trait composition.~~ Furthermore, individual species have been shown to demonstrate differing traits depending on external stresses. *Populus nigra* trees were found to be smaller, have greater flexibility, and had a higher number of structural roots at a bar head when compared to a bar tail (Hortobágyi et al., 2017)(Hortobágyi et al., 2017). Further work demonstrated that the trees located at the bar head were less effective at trapping sediment when compared to those at the bar tail (Hortobágyi et al., 2018). This highlights that ~~in certain examples,~~ the morphological response to a-vegetation may be harder to identify from taxonomic ~~approaches alone, with rather than~~ traits-based ~~data helping to unpick the processes that are occurring~~ approaches.

140 Research into effect traits and their geomorphic influence has received relatively less attention as traits concepts have only recently started to be explored ~~in fluvial research. However, as noted by Corenblit et al. (2015), the interactions between plant traits and fluvial systems are linked, with hydraulic conditions affecting plant establishment and survival, and with plant traits affecting flow and subsequent morphology within fluvial research.~~ Temporally, changes in the dominant traits can lead to changing morphology (Manners et al., 2015), whilst spatially the location of dominant traits has been shown to alter morphological response, with combinations of different ~~guilds/functional groups~~ adding to the complexity (Hortobágyi et al., 2018). However, ~~guilds/functional groups alone~~ cannot explain all the variation in topographic response, with different groups ~~of traits~~, in different locations, under different hydraulic conditions, exhibiting different topographic responses (Butterfield et al., 2020).

150 1.3.1.2. Hydraulically Relevant Traits

Not all vegetation traits are equally relevant when considering direct relationships between vegetation, river flow, and morphology. Moreover, not all traits can be obtained ~~directly~~ from remote sensing techniques, a necessary requirement when upscaling to larger domains. Below we briefly summarise vegetation traits that are ~~highly~~ relevant to fluvial environments and which have the potential to be captured via remote sensing techniques, ~~thereby allowing the upscaling of any developed methods of characterisation.~~ These are based off Table 2 in Diehl et al. (2017a) which highlights the morphological effect of vegetation traits on geomorphic form.

160 Both plant height and frontal area are key traits which influence momentum exchange in river flows. The height of a plant will alter the extent of interaction it has with flow at various stages, whilst the ~~submerged~~ frontal area ~~of the submerged plant structure~~ will impact the drag exerted on the water column (Nepf and Vivoni, 2000; Järvelä, 2004; Wilson et al., 2006). ~~Using 2D frontal area to describe the complex structure of plants is not without limitations, and the possibility of using 3D data has~~

165 offered improvements in this regard (Whittaker et al., 2013; Vasilopoulos, 2017). The frontal area of a plant will vary under
different hydraulic conditions, making flexibility an important trait when investigating morphological response. ~~Not~~
170 ~~accounting for flexibility can limit the applicability of study results (Sand Jensen, 2008; Whittaker et al., 2013), with~~
~~differences in foliated and non-foliated vegetation deforming at different threshold velocities (Wilson et al., 2003; Järvelä,~~
~~2002b). Likewise, differences in woody and non-woody stems for plants of similar shape will influence their flexibility, with~~
~~woody stems requiring a higher flow rate for deformation to occur (O'hare et al., 2016; Sand Jensen, 2003). Both differences~~
175 ~~in foliated and non-foliated vegetation as well as woody and non woody stems alter the thresholds in velocity at which~~
~~deformation occurs (Wilson et al., 2003; Järvelä, 2002a; O'hare et al., 2016; Sand-Jensen, 2003), modifying a plants effective~~
~~frontal area.~~ However, the ability to obtain vegetation stem flexure directly from remote sensing is currently not possible, yet
leaf area from remote sensing does show potential, and taxonomic approaches may better identify the 'woodiness' of a species.
Likewise, the vertical distribution of vegetation is important in determining the interaction between foliage and flow stage
(Lightbody and Nepf, 2006; Jalonen et al., 2012), which can be obtained from remotely sensed data.

180 At patch scales, the density and configuration of plants can impact the resultant drag ~~effects.~~ ~~Although this is an extension of~~
~~the individual plant based methods within ecological research, including density and configuration allows for the impact of~~
~~multiple plants on drag to be accounted for.~~ The non-equivalence between the drag induced by individual plants ~~and stems~~
~~and compared to~~ those in bulk vegetation requires the inclusion of bulk factors ~~in to~~ into vegetation analysis (James et al.,
185 2008). Higher densities of plants will lead to an increase in drag, with differences in the arrangement and density of patches
causing variation in the resultant reduction in water velocities (Järvelä, 2002a, 2002b; Kim and Stoesser, 2011; Sand-Jensen,
2008). ~~The resultant changes in flow patterns through patches of higher density vegetation can subsequently increase scour~~
~~around individual stems (Follett and Nepf, 2012), highlighting the need to account for plant spacing when examining changes~~
~~in morphology. At the reach scale, functional groups have a combined role, highlighting the need to account for plant spacing~~
190 ~~when examining changes in morphology, which remote sensing is capable of achieving. At the reach scale, functional groups~~
~~have an aggregated response~~ in modulating scour or deposition, and resultant planform morphology. Vegetation dynamics
have been described using traits-based frameworks ~~previously~~ in fluvial systems (Diehl et al., 2017a; Diehl et al., 2018;
Butterfield et al., 2020), with a wealth of studies showing the ~~wider~~ impact that vegetation has on planform morphology and
erosion in flumes (Van Dijk et al., 2013; Coulthard, 2005; Bertoldi et al., 2015), modelling studies (Oorschot et al., 2016;
Crosato and Saleh, 2011), and field based research (Bywater-Reyes et al., 2017; Diehl et al., 2017b).

195 Whilst we have focused on hydraulically relevant traits that can be measured using remote sensing techniques, Diehl et al.
(2017a), present others which cannot ~~be easily be~~ obtained from the remote sensing techniques outlined below. Factors such
as plant biomass, buoyancy, and root architecture are all outlined as having a role in affecting subsequent morphology (Sand-
Jensen, 2008; Abernethy and Rutherford, 2001; De Baets et al., 2007). This highlights the potential role of taxonomic

approaches alongside the measurement of structural data, to both capture the variability where possible, and enhance this with wider datasets on traits that cannot be remotely sensed but are still relevant to morphology.

1.4.1.3. Remote Sensing for Trait Data Collection

200 Although ~~many of these~~ some traits are inherently measurable in the field, many of them are not obtainable from current remote sensing methods. Direct trait extraction for riparian vegetation from airborne (i.e. large scale) remote sensing has not yet been ~~utilised to enhance~~ used within eco-geomorphic studies. Currently, ~~the~~ collection of trait data relies on ~~direct~~ ground-based field surveys using quadrat or transect sampling and lab analysis, or species ~~are being~~ identified in the field and traits ~~taken~~ inferred from ~~databases~~ lookup tables; such as the TRY database (Kattge et al., 2020). ~~Methods are often dependent on site access, species richness, and variation within the study area (Palmquist et al., 2019), utilising methods such as quadrat surveying or transect sampling.~~ This technique is effective for establishing traits but is limited by the spatial extent of ground coverage. ~~Some variables inevitably require databases to avoid substantial disturbance, such as root characteristics (e.g. Stromberg and Merritt, 2016; Aguiar et al., 2018; Baattrup-Pedersen et al., 2018). However, it is known that a single species can display different traits depending on their position relative to the channel (Hortobágyi et al., 2017; Hortobágyi et al., 2018).~~

205 Therefore knowledge of a plants location, which can be obtained from remote sensing data, alongside using plant traits databases is important for successfully utilising such traits based analysis in the fluvial domain. Although efforts have been made to utilise remote sensing methods to infer traits in other fields (Anderson et al., 2018; e.g. Valbuena et al., 2020; Zhao et al., 2022), these typically relate to vegetation height and volume.

215 ~~In~~ Within fluvial research, multispectral imagery ~~can be used~~ has been collected to determine ~~species~~ plant species which are then used to identify dominant traits, via supervised and unsupervised classifications, ~~with good overall accuracy, which can then be used to help assume dominant traits (Butterfield et al., 2020).~~ Outside of fluvial research there is an increasing awareness of the potential of remote sensing methods to help drive the scalability of functional traits as an analysis framework, especially in relation to physical traits such as plant height, leaf area index, phenology, and biomass ~~the fluvial domain, several efforts have been made to utilise remote sensing methods for trait extraction, using a mix of terrestrial, airborne, and satellite platforms (Abelleira-Martínez Anderson et al., 2016; 2018; Valbuena et al., 2020; Zhao et al., 2022; Aguirre-Gutiérrez et al., 2021; Abelleira Martínez et al., 2016), yet considerable.~~ However, limitations still remain despite these efforts due to the uncertainty in relating spectral and physical properties to functional traits (Houborg et al., 2015). ~~Upscaling localised high resolution data is possible however, for example from TLS (Terrestrial Laser Scanning) to large scale ALS (Airborne Laser Scanning) data (Manners et al. (2013).~~

225

Yet, considerable advances continue to be made in using remote sensing to monitor riparian vegetation at a range of scales. Advances in UAV (Uncrewed Aerial Vehicle) remote sensing can offer a way of bridging the scales from ground surveys to

larger extents. UAV data collection allows high resolution imagery and active remote sensing methods such as laser scanning to be conducted on large reaches relatively easily (Tomsett and Leyland, 2019), increasing coverage and providing a middle ground for relating local to large scale data. Multispectral cameras have already helped to improve the classification of vegetation from UAVs (Al-Ali et al., 2020), ~~and active UAV LS (UAV Laser Scanning) has also been shown to be comparable in estimating tree structures to TLS methods (Brede et al., 2019). Such methods therefore with active UAV-LS (UAV Laser Scanning) being shown to be comparable in estimating tree structures to Terrestrial Laser Scanning (TLS) methods (Brede et al., 2019; Hillman et al., 2021), and a combination of both techniques helping to improve tree crown delineation and biomass estimates (Dersch et al., 2023; Lian et al., 2022; Dash et al., 2019). TLS has become the benchmark technique from which to obtain highly accurate vegetation data (Bywater-Reyes et al., 2017; Jalonen et al., 2015; Lague, 2020), yet still suffers from issues of occlusion and limited spatial extent in comparison to mobile techniques. Airborne Laser Scanning (ALS) can be used to classify different vegetation regimes, classifying different woodland types (Stackhouse et al., 2023) and identifying differences in species using intensity data (Donoghue et al., 2007), but obtaining temporally relevant data at adequate point densities is challenging.~~

~~The survey techniques outlined above present an opportunity to not only classify vegetation by types and assign them to functional groups, but also to define these very groups based on characteristics acquired directly from remote sensing directly, before upscaling them to reach scale classifications. Moreover, a key advance in using UAV based methods for collecting vegetation data, is the spatial resolution at which functional groups can be discretised and the temporal resolution which can be achieved by undertaking multiple repeat surveys. The potential to capture evolving 3D data through time (which we refer to Such surveys can allow for both leaf-on and leaf-off conditions as well as the 4th dimension herein) provides arguably the biggest advantage emergence of using UAV-based methods to collect data perennial vegetation, avoiding the need to make any assumptions about variability through the phenological cycles by collecting this information directly cycle. Consequently, identifying whether it is possible to obtain trait data from various remote sensing sources, upscale these to reach scale metrics, and examine links to geomorphic activity, is underexplored.~~

1.5.1.4. Aims

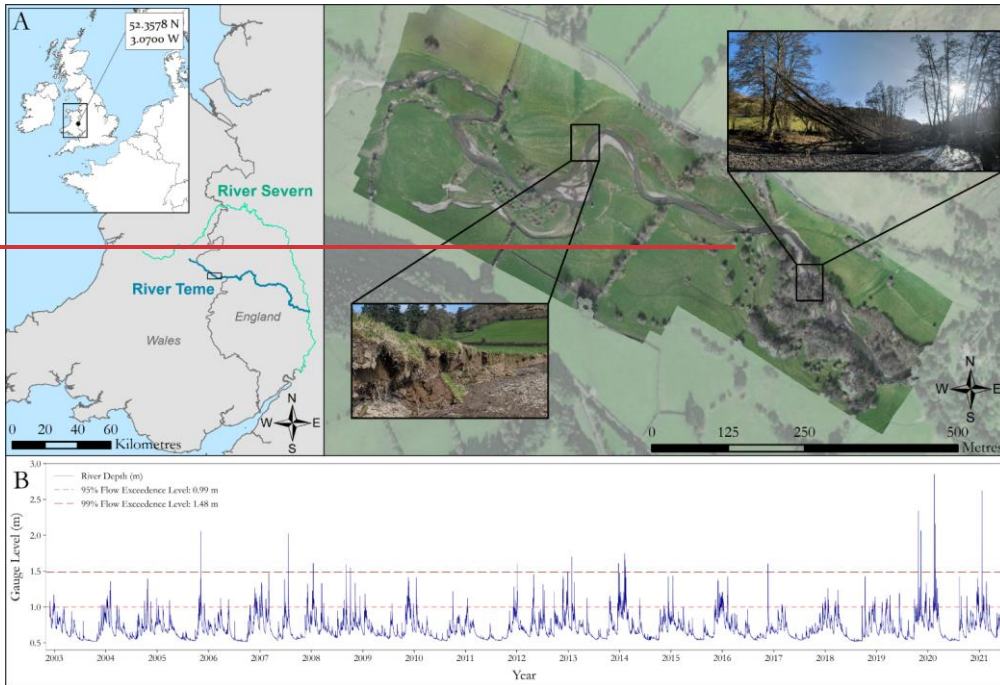
The aim of this research is to use UAV derived and terrestrial 3D datasets to ~~develop a workflow and methods which are able to extract relevant plant traits which can be used to assess to explore~~ the spatial and temporal (i.e. 4D) variation and importance of eco-geomorphic interactions on a UK river system. This is achieved using the following specific objectives:

1. ~~Identify~~ Develop a methodological workflow to identify and select hydraulically relevant traits ~~which can be~~ extracted from high resolution remote sensing data.
2. Establish the presence of functional groups (those with similar traits) for the river reach using exploratory analysis and machine learning.

3. ~~Compare~~Examine links between the spatial ~~extent of these~~variation in functional groups ~~to~~and morphological change over the study~~across a two year~~ period to ~~establish~~identify any eco-geomorphic feedbacks~~– that may be present~~.
4. ~~Utilise the structural data to establish how the influence on flow of different functional groups varies seasonally and annually, comparing this to observed erosion and deposition.~~

2. Study Site

The study site is located on the upper course of the River Teme on the English-Welsh border in the UK (Figure 1A). The ~~study area~~reach consists of two distinct ~~reach~~sections; an upstream section consisting of open grassland with patches of heterogeneous vegetation, and a downstream section which flows through denser vegetation and woodland. The River Teme is a highly mobile, gravel bed river within an alluvial floodplain which exhibits numerous ~~historic~~ avulsions, typical of many UK rivers. There is active lateral erosion of the channel, depositional gravel bar features, and woody debris dams across the study site (Figure ~~1A~~1B). The reach has typically low flows (Figure ~~1B~~1C), with an average depth of 0.69 m (+/- 0.15 m) throughout the year with slightly higher average flow depths in the winter months (November – February, 0.79 m +/- 0.15 m). 95% of river depth has been below 0.99 m and 99% of the flow depth has been below 1.48 m. The largest recorded river depth was 2.85 m on the 16th February 2020 during ~~Storm~~Storm Dennis.



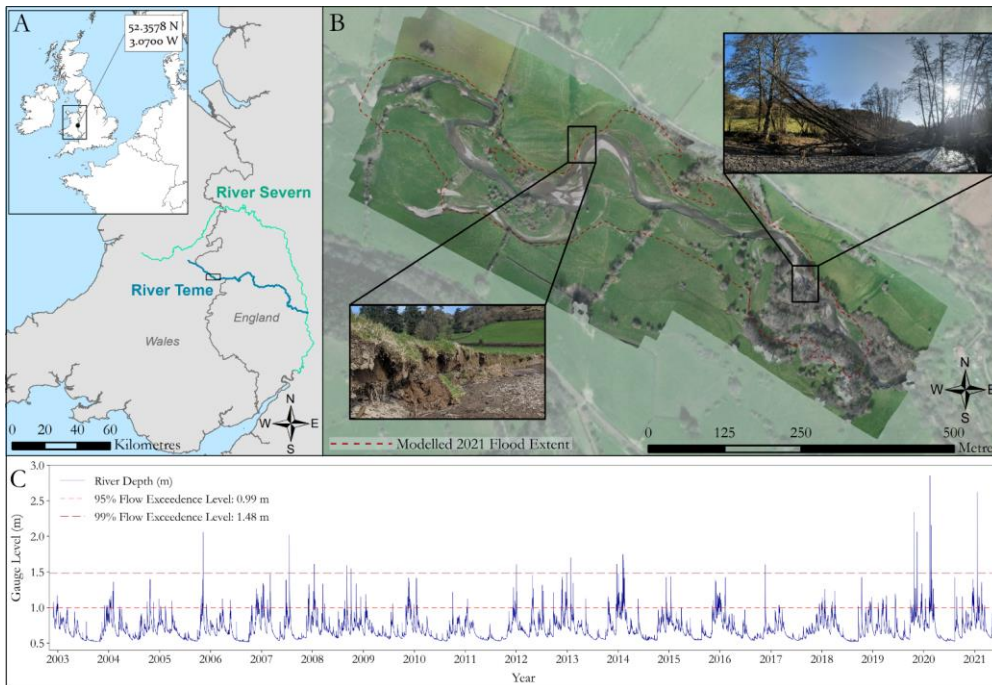


Figure 1 Study Site of the River Teme and the long term water level at the Knighton gauge station 3km downstream. **A)** Study Site Location on the River Teme, UK. **Inset B)** Plan view of the reach with inset images showing active bank erosion and a large debris dam caused by falling trees. **The red dashed outline indicates the flood extent modelled within this study.** Orthoimagery collected February 2020 and background imagery provided by **ESRI (2021).** **B)** River Gauge Level **Esri (2021).** **C)** River gauge level at the Knighton monitoring station ~2 km downstream from study reach (data available from 2002 – present, operated by the UK Environment Agency).

285 3. Methods

3.1. Field Collection of High Resolution 4D data

A series of six high resolution UAV-LS (UAV Laser Scanning) and UAV-MS (UAV Multispectral) surveys were collected over the entire reach shown in Figure 1 from February 2020 until June 2021, capturing all seasonality. To complement these flights, a single Terrestrial Laser Scanning (TLS) survey using a Leica P20 was undertaken of vegetated and bar sections in July 2020 to gain a benchmark ultra-high-resolution dataset for characterising small herbaceous vegetation, co-registered to an accuracy of +/- 0.007 m with georeferenced scan targets. A-UAV-RGB (Red, Green, Blue) survey was surveys were also undertaken during overbank flow on the falling limb of Storm Dennis in February/September 2020, to identify the flood extent

for classification validation. Table 1 summarises the survey dates, extents, data collection methods, and point density for UAV-LS and GSD (Ground Sampling Distance) for UAV-MS. A detailed outline of the UAV based sensor set up, processing routine and accuracy assessment can be found in Tomsett and Leyland (2021). All data was processed in the WGS UTM Zone 30N coordinate system.

Table 1 Data collection methods, extent, and point density for each survey date. TLS point density is based on the resultant point cloud after registration. [‡]UAV-LS point density is determined after cleaning of the raw clouds has taken place. Ground Sampling Distance (GSD) is the resolution of the resultant orthomosaics. UAV-LS point density is taken once cleaning of the raw clouds has taken place.

Date	Survey	Sensor	Point Density/GSD [‡]
06/02/2020 (Winter)	Whole Reach	UAV-LS	778 m ⁻²
		UAV-MS	0.04 m GSD
18/02/2020 (Winter)	Whole Reach	UAV-RGB	0.02 m GSD
		UAV-LS	810 m ⁻²
16/07/2020 (Summer)	Subsection	<u>UAV-MS</u>	<u>0.04 m GSD</u>
		<u>TLS</u>	<u>16,000 m⁻²</u>
		<u>UAV-LS</u>	<u>762 m⁻²</u>
<u>14/09/2020</u>	<u>Whole Reach</u>	UAV-MS	0.04 m GSD
		TLS	16,000 m⁻²
		<u>UAV-LS</u>	<u>762 m⁻²</u>
14/09/2020 (Autumn)	Whole Reach	UAV-MSRGB	0.0402 m GSD
		UAV-LS	791 m ⁻²
14/04/2021 (Spring)	Whole Reach	UAV-MS	0.04 m GSD
		UAV-LS	804 m ⁻²
03/06/2021 (Summer)	Whole Reach	UAV-MS	0.04 m GSD

3.2. Vegetation Functional Trait Extraction

The workflow developed to extract plant functional traits consisted of five steps: (1) Separation of individual plant point clouds from the UAV-LS data from February 2020 and TLS data from July 2020, (2) Analysis of these individual clouds to extract metrics related to their traits, (3) Separation of plants into functional groups adapted from Diehl et al. (2017a)_‡ based on similar

traits, (4) Identification of functional group reach scale properties from UAV-LS and UAV-MS datasets for reach-scale classification inputs from 2020, and (5) Use of an object-based random forest classifier to determine the spatial discretisation of these functional groups for both 2020 and 2021. These steps are outlined in the following sections and are shown as a processing workflow in Figure 2 to provide context in relation to which surveys contributed to each element of the analysis. Figure 2 also shows how the resultant functional groups are used in conjunction with the morphological change detection.

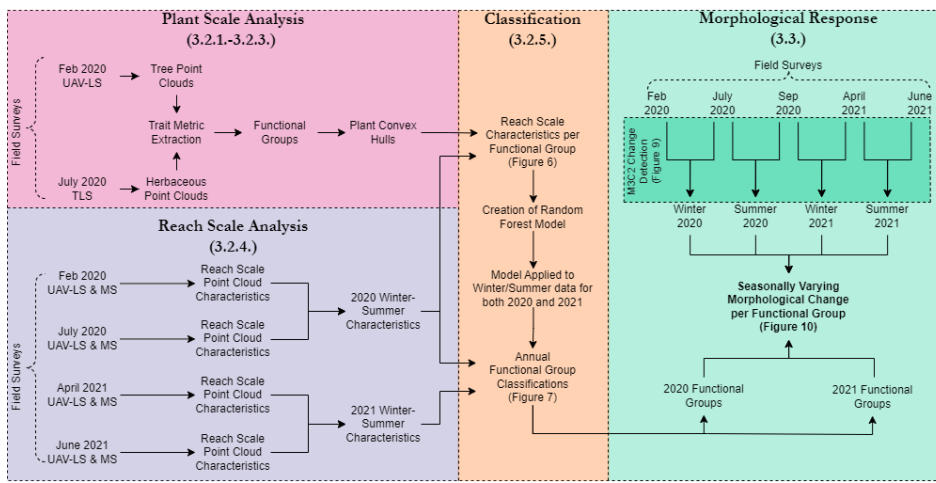


Figure 2 An overview of the workflow used to process collected field data (Table 1) through to analysis of morphological change for each functional group. Each colour-block indicates a different stage of the analysis which corresponds to the numbered sections that follow.

3.2.1. Point Cloud Segmentation

A number of automatic methods exist to classify very dense point cloud scenes into different groups (e.g. Brodu and Lague, 2012; Zhong et al., 2016). However, the majority of these are designed for very-ultra-high-resolution TLS datasets, rather than UAV-LS (see Table 1 for density metrics) and so here-a semi-automated approach was employed. Smaller vegetation whose, where the structural composition cannot be fully resolved from UAV-LS data were, was analysed from the summer/July 2020 TLS survey, whereas larger vegetation was analysed in leaf-off conditions from the February 2020 survey. Automatic classification of ground/non-ground points was performed using the progressive morphological filter in the LidR package (Roussel et al., 2020)(Roussel et al., 2020) before manually segmenting in CloudCompare (<https://www.danielgm.net/cc/>) to create individual plant models (Figure 23, Raw Point Cloud).

For the herbaceous plants in the TLS data, leaves and flowering parts were manually removed from the clouds so as not to influence with the quantitative structural modelling (QSM; see 3.2.2). This was done based on field images and the structural

appearance of the clouds to leave just the structural components. Although foliage has previously been shown to be important, (Järvelä, 2002a; Whittaker et al., 2013), for the methods used herein it could not be fully resolved due to insufficient point densities ~~in comparison to ground-based TLS.~~ Any statistical outliers were then detected and removed ~~from the dataset using the in-built tools within CloudCompare,~~ identifying points >2.5 standard deviations above the mean separation distance between points within the segmented cloud. This process was repeated for plants ~~in both TLS scan locations found within the TLS scans of the study site,~~ resulting in a sample dataset consisting of 37 herbaceous plants. Plants that were selected ~~in from~~ the ~~main~~ TLS point cloud ~~that~~ represented complete vertical profiles to minimise the effect of shadowing from different scan angles.

Tree segmentation also ~~used~~ consisted of a combination of manual and automatic classification, based on surveys undertaken in leaf-off conditions, ~~exposing to expose~~ the full ~~internal~~ tree structure. 24 trees were selected from across the reach, representing a range of structures and sizes from which complete models could be created. ~~Initial separation of ground and vegetation points was performed using a progressive morphological filter.~~ Trees were ~~then~~ manually extracted; prior to interactive filtering using a number of statistical measures; local volume density helped to separate points distinct from the main tree woody structure, whilst linearity metric filters (how aligned points are within a set radius) removes points that are highly complex or not part of the main tree structure. The statistical outlier removal tool and a final manual check can then be used to remove any remaining points ~~which are not part of the main tree structure.~~ This resulted in a point cloud of predominantly large branches, with a clearer structural profile as can be seen in Figure 23 (*Filtered Point Cloud*). The thresholds for separating individual trees are size, structure, and point density dependent, hence the need for interactive selection. Although this adds an element of user bias as to what is deemed a 'main' branch, the lower density of UAV-LS scans makes user input necessary before reconstructing vegetation models (Brede et al., 2019).

Shrubs and grasses whose structure could not be fully resolved from the UAV-LS or TLS data were not analysed for traits extraction. Grasses are typically too short to remotely sense with high degrees of confidence, and the complex and extensive nature of the branching network of shrubs would require several TLS scans per plant, with numerous plants needing to be surveyed to get a reliable trait description. ~~As a result, point clouds for shrub classes were used for classification training, and frontal area and density calculations.~~ (Vasilopoulos, 2017). As a result, point clouds for shrub classes were only used for classification training, frontal area, and density calculations.

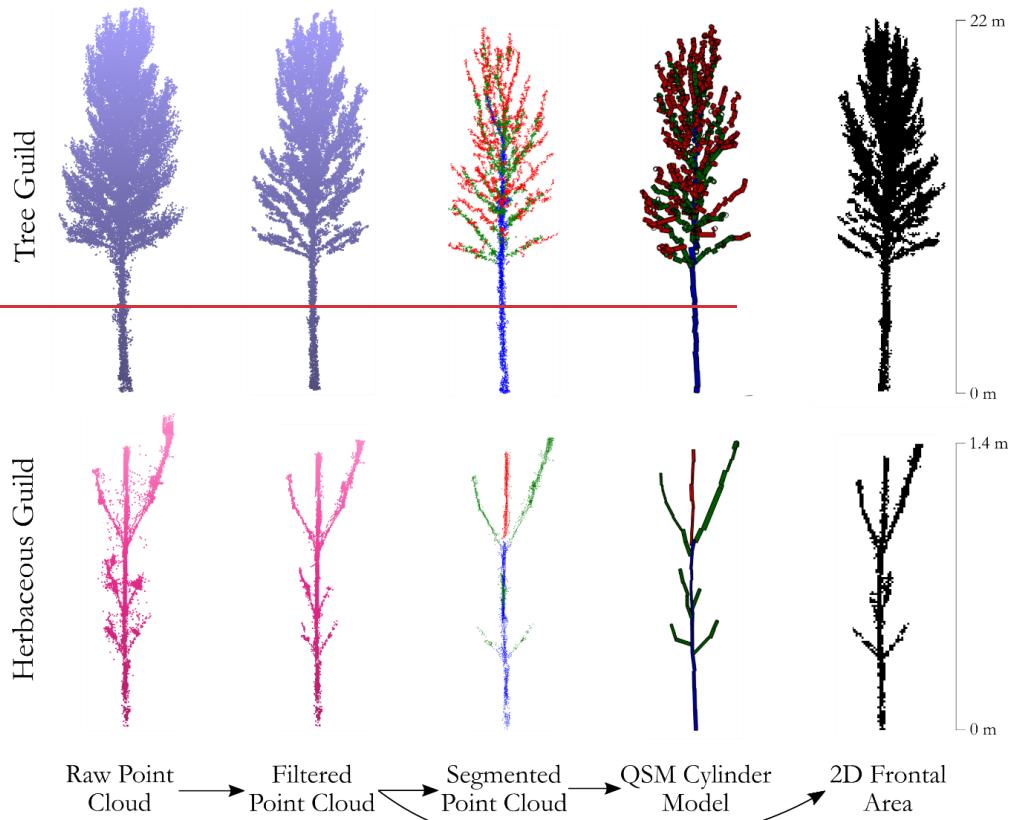
3.2.2. Trait Metric Extraction

The hydraulically relevant traits collected were based on those noted within Diehl et al. (2017a) ~~that which~~ could also be measured using the remote sensing methods available to us within this study. These were; plant height, number of branches, maximum branching order, stem ~~diameters, plant volume, frontal area, and plant density.~~ ~~For the reconstruction of vegetation~~

stems into cylindrical models, the open source TreeQSM method was applied to the partitioned UAV-LS and TLS derived vegetation data (Brede et al., 2019). diameter, plant volume, frontal area, and plant density.

For the reconstruction of vegetation stems into cylindrical models, the open source TreeQSM method (Raumonen et al., 2013)

365 was applied to the segmented UAV-LS and TLS derived individual plant data from 2020 as outlined above. TreeQSM utilises 'patches' to determine connected points in the vegetation cloud, before growing the tree structure by joining patches together to form a complete model (Raumonen et al., 2013). These are created using user defined initial patch sizes to adjoin points, before refining the patch sizes using minimum and maximum sizeslimits to create a complete model. This allows the coarse branch structure of the tree to be identified (Figure 23, *Segmented Point Cloud*). Sections are then generalisedreconstructed as
370 cylinders, both for computational efficiency and because they provide a robust representation of trees (Raumonen et al., 2013). The cylinders are then used to describe the overall structure and properties of the individual plant (Figure 23, *QSM Cylinder Model*). A full method description can be found in Raumonen et al. (2013). QSM methods have been noted to overstate the volume of smaller branches and are sensitive to noise in the data alongside variable point density (Fang and Strimbu, 2019; Hackenberg et al., 2015). However, QSM reconstructs treeplant structures in a manner which resolve many of the hydraulically
375 relevant vegetation traits, making it a suitable approach for this research.



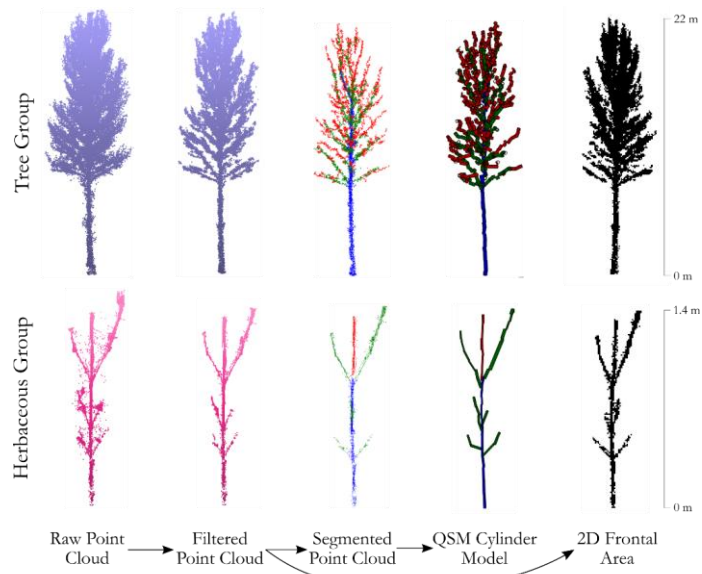


Figure 23 Vegetation trait extraction, from an individual raw plant point cloud to a cylindrical model and frontal area. The process is demonstrated for two extracted vegetation point clouds, a large tree within the study reach collected from UAV-LS data, and a small-perennial on the central bar collected from TLS, note the difference in scales. The segmented point cloud is coloured by branching order from blue to green to red, with the cylinders coloured in the same manner. The 2D frontal areas are based on the filtered point clouds rather than the segmented point clouds or QSM cylinder models, and as such these steps are not required to compute the frontal area data.

385 Patch diameters (which are used to determine adjacent points within the same tree) were chosen following a parameter sensitivity exercise, with the range of values initially based around those of Raunonen et al. (2013) and Brede et al. (2019) for TLS and UAV-LS approaches respectively. A visual assessment was performed to identify parameters that created models similar to the observed -vegetation structure- in the point cloud, due to the lack of reference data. After testing for the optimum patch sizes for reconstruction, the TLS scans of herbaceous vegetation initial patch diameter was set at a size of 0.005 m, with the second patch diameter minimum and maximum sizes of 0.002 and 0.01 m. The minimum cylinder radius was set to 0.005 m, prescribing the smallest detectable branch structure of the extracted herbaceous plants. For the UAV-LS derived tree data, the initial patch diameter was 0.2 m, with the second patch diameter minimum and maximum sizes of 0.1 and 0.5 m. The minimum cylinder radius was 0.1 m, based on manual measurements of tree branches within the point cloud that were detectable. For each individual plant model the cylinder reconstruction and variable extraction was repeated ten times. As the modelling begins at a random location each time, the start point can affect the results, and so multiple averaged simulations

~~provides~~provide a more ~~accurate~~representative solution. The modelling produces a number of metrics, but for this study hydraulically relevant traits of plant height, number of branches, stem diameter, volume, and maximum branching order, were collected. For each metric of interest, the average value and standard deviation of these values are taken from the ten runs.

400 The frontal areas of all segregated vegetation clouds were extracted alongside the construction of the cylinder models, based on the 2D methods described by Vasilopoulos (2017). For each discretised filtered plant point cloud (Figure 23, *Filtered Point Cloud*), the data was flattened from 3D to 2D by collapsing the data along a single horizontal dimension on a regular grid (Figure 23, *2D Frontal Area*). The grid resolution was set at half the width of the minimal detectable feature resolved by the QSM modelling; ~~0.005~~0.025 m for the TLS derived herbaceous plants and UAV-LS 0.05 m for UAV-LS derived trees. Each
405 plant was flattened along the X and Y axis respectively, with an average frontal area taken.

~~Plant density was calculated as follows. For herbaceous vegetation and shrubs, sections of vegetation were discretised from TLS and UAV-LS data respectively for analysis. A raster surface of these discretised zones was then created (0.05 m resolution for herbaceous and 0.2 m for shrubs) and a local maximum filter used to identify the top of individual plants, similar to the procedures used to delineate individual trees in dense canopies. In the absence of manually collected field validation data, to assess the ability of the UAV-LS to capture vegetation properties, and for the QSM to produce reliable models, a series of checks were undertaken. First, UAV-LS tree heights and DBH from February 2020 and April 2021 were compared to trees that were also captured in the TLS scans from July 2020. It is assumed that differences in tree height and DBH between these surveys due to the temporal offset would be negligible. This provides an estimation of how well UAV-LS captures tree properties compared to the benchmark high resolution techniques (Douss and Farah, 2022; Chen et al., 2020)(Kankare et al., 2013; Hillman et al., 2021; Calders et al., 2015; Brede et al., 2019). The number of individual plants was calculated, and divided by the total discretised area, to provide plant density. For larger vegetation, where the trunks could be reconstructed, the procedure was very similar, but as canopy detection can be challenging in densely vegetated regions, the point cloud was inverted before running the local maximum model to identify the locations of tree trunks. A 0.2 m raster surface was used for this and the number of trunks was counted to provide both sets of tree density data.~~

410
415
420

~~. For both the herbaceous and tree plants within the QSM analysis, the modelled plant heights and DBH were compared to measured values from each plants point cloud, with DBH being measured across two perpendicular axis to obtain a mean diameter for the point cloud. Finally, available databases and the wider literature were used to ensure values were within the expected range for each species measured at other sites (see section 4.2.1).~~

425

3.3.3 Identification of Functional Groups

For the separated individual plant point clouds, each were assigned to a functional group -adapted from those outlined in ~~O'hare et al. (2016)~~O'hare et al. (2016) and Diehl et al. (2017a). These groups were grasses, short branching herbs, tall single stemmed

430 herbs, shrubs and bushes, low DBH trees, and high DBH trees. As discussed previously, shrubs and grasses were not identified using trait extraction. Short branching herbs and taller single stemmed herbs were separated due to the likely ~~discrepancies~~ variability in flexibility, branching architecture, and height, all of which interact differently with flow. ~~Woody~~ Large woody vegetation was split into two functional groups, those with high diameter at breast height (DBH) that had low density of ~~trunks~~ plants, and those with lower DBH that had a higher ~~trunk~~ plant density, to account for the different interactions with overbank flow.

435 To assess whether remotely sensed data could separate out plants into their functional groups in a statistically robust way, a Principal Components Analysis (PCA) was undertaken to identify the variables which explained most variation within the derived trait metrics. The metrics used for the PCA were those obtained from the QSM and frontal area calculations outlined ~~previously~~ above, which were normalised to remove the influence of different scales (Alaibakhsh et al., 2017). The principal components identified were used to inform the classification of reach scale functional groups, identifying those variables that most explained the variation between groups. The PCA was performed separately on the two ~~herb~~ herbaceous groups and the two woody groups, as although height would clearly be ~~an obvious~~ dominant variable between these two groups, it would not necessarily be one within the groups. All of the herbaceous point clouds from the ~~summer 2020~~ TLS survey were used in the ~~herb~~ herbaceous group PCA, and all the high and low DBH ~~tree~~ tree point clouds from the ~~winter 2020~~ UAV-LS data were included in the woody group PCA.

3.2.4. ~~Linking Traits to~~ Land Cover Metrics at the Reach Scale Metrics

450 To scale the analysis from individual plants to the entire reach level, a method of linking plant scale traits to ~~broader~~ reach scale data is required. Convex hulls representing the spatial extent for each ~~plant scale~~ vegetation point cloud ~~extracted and~~ analysed above were used to define the regions from which UAV-LS and UAV-MS data were extracted. For small herbaceous vegetation, this was buffered by 0.25 m to account for any misalignment between TLS and UAV-LS clouds. For tree vegetation polygons this buffer was increased to 1 m to incorporate peripheral branches and leaves removed during point cloud filtering. ~~Polygons~~ 11 polygons for ~~small branching trees and large shrubs and bushes~~ were created based on field notes ~~from various surveys~~ and photographs ~~from the summer surveys~~, their outlines in the UAV-LS point clouds, and UAV-MS imagery. ~~A total of~~ Similarly, 11 polygons were ~~created for this combined functional group category, with 11 made~~ defined for grasses. ~~In addition to these vegetation functional groups, 8 polygons for water classes, and 5 for a combined gravel bars and bare earth-class were also created using the same technique to classify the remaining land cover.~~ Within these polygons, ~~multiple seasonal~~ leaf-on and leaf-off variables were extracted for scaling ~~local~~ plant scale functional group identification to reach scale classification.

460 The structural characteristics of the ~~reach scale~~ point ~~cloud~~ clouds were extracted through TopCAT (Brasington et al., 2012), obtaining the standard deviation, skewness, and kurtosis over a sampled grid at 1 and 4 m resolutions, the latter to account for

larger vegetation footprints. The 4 m resolution grid only considered points classified as vegetation ~~in the initial 'ground/other'~~
~~point clouds~~ to remove ground points ~~from further analysis~~. To extract a Canopy Height Model (CHM), a bare earth digital
terrain model (1 m resolution) was subtracted from a ~~0.25 m~~ digital surface model ~~(0.25 m resolution)~~ incorporating the
465 vegetation points. The Normalised Difference Vegetation Index (NDVI) across the reach was calculated using the red band
along with both the red-edge and near-infrared bands of the MicaSense orthomosaic images to produce two separate NDVI
layers. As the red-edge can be used to separate out vegetation signatures, using a combination of both was expected to help
differentiate plants with similar structural but different spectral properties. ~~Analysis of structural and spectral data was~~
~~performed for each of the surveys to gain an insight in to how these properties vary temporally.~~ (Schuster et al., 2012; Guo et
470 al., 2021). For each of the vegetation ~~polygons~~ ~~convex hulls~~, the attributes of ~~each of these the structural and spectral~~ layers
for ~~each season~~ ~~leaf-on and leaf-off conditions~~ were extracted ~~using zonal statistics~~. The mean and standard deviation for each
attribute for each survey were then calculated across the different functional groups for use in the classification model.

3.2.5. Reach Scale Functional Group and Land Cover Classification

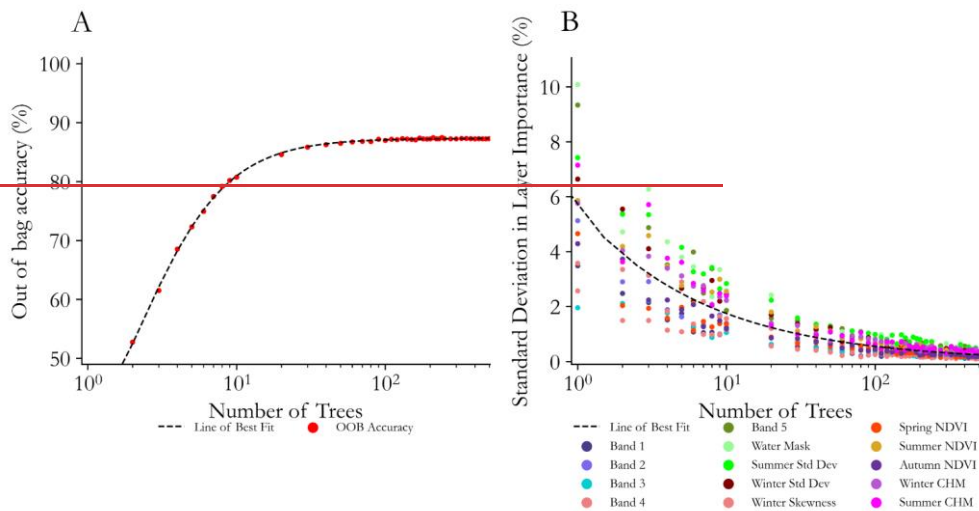
To ~~transition from plant~~ scale ~~from~~ groups created from individual UAV-LS and TLS ~~derived plants, clouds~~ to ~~the entire~~ reach
475 ~~scale analysis~~, an object-based random forest classification was undertaken. Object-based approaches overcome some of the
issues of variation and complexity in high resolution images (Myint et al., 2011), improving continuity in the results (Duro et
al., 2012; Wang et al., 2018). The RGB bands from the multispectral camera and the CHM were combined to create a 4-layer
image from which to ~~classify/identify~~ distinct objects in summer imagery for ~~both~~ 2020 and 2021. The Felzenszwalb Algorithm
was applied which uses graph based image analysis to segment an image into its component parts based on the pixel properties
480 (Felzenszwalb and Huttenlocher, 2004). This results in regions within the image being grouped ~~basebased~~ on them having
similar properties according to the input layers, avoiding the salt and pepper effect found in traditional pixel by pixel
classification approaches (Wang et al., 2018).

485 **Table 2 Description of functional groups and land cover classes used for training the random forest classifier, showing the number
of training objects from the image segmentation for 2020 imagery, and the training area size.**

<u>Functional group/Land cover</u>	No. of Training Objects	Training Area Size (m ²)
Grasses	93	321
Branching Herbs	15	25
Single Stemmed Herbs	16	29
Branching Shrubs	135	388
Low DBH Trees	158	876
High DBH Trees	62	238
<u>Gravel Bars and Bare Earth</u>	122	641
Water	41	157

In total, 644 training objects were identified for the 2020 summer imagery, ~~within~~with the previously discretised vegetation convex ~~hull regions with hulls having~~ multiple ~~training~~ objects present within each ~~training~~ sample (Table 2). A random forest classifier was then trained using this 2020 data, ~~having proved an effective machine learning technique (Adelabu and Dube, 2015; Chan and Paelinckx, 2008; Adam and Mutanga, 2009), with the layers that were deemed to distinguish between the different functional groups. The structural and spectral datasets created in 3.2.4. being~~were used as the input and ~~to~~ train the model, alongside an additional water mask ~~included~~layer created from the multispectral imagery to ~~reduce errors associated with~~account for varying flow ~~stage. As the distinguishing features of~~stages. Data from leaf-on and leaf-off conditions were used for each ~~functional group required the inclusion of~~years classification, with an annual map being constructed. This was ~~chosen due to the need for~~ both summer and winter data, ~~an annual classification as opposed to a seasonal one, is undertaken to classify different functional groups.~~ This helps to improve confidence in the classification where variation in reach scale metrics happen both between groups and between seasons. ~~Although leaf-on and leaf-off data with no geomorphic change between surveys would have been favourable, the combination of datasets where geomorphic change had occurred is unavoidable based on the survey dates.~~

An analysis of model accuracy vs number of forests showed a convergence of accuracy above 100 forests and a reduction in band importance variability above 300 forests (~~Figure 3).~~ Higher variation in band importance ~~suggested~~suggests that the number of trees ~~was~~is influencing the likelihood of an optimal solution. This random forest classification was then applied to the remaining ~~unclassified~~ objects within the reach for 2020, and also for all objects in the ~~segmented~~ 2021 data.



505 **Figure 3 Random forest classifier out-of-bag accuracy and variations in band importance for functional group classification. A) Out of bag accuracy scores for different numbers of trees used within the random forest classification, showing a distinct levelling off in accuracy after ~100 trees are used. B) The standard deviation in individual band importance across 10 sample runs to identify at what number of trees band importance becomes consistent across all runs, in this instance around 300 trees.**

510 Due to the limited number of extracted samples from the point clouds, there were not enough training samples to split into a training and test dataset. The multi-tree approach of random forests is constructed on a sample of the dataset and as such can be tested against itself to determine an out of bag accuracy score. It also successively adds and removes bands to determine the band importance in the classification (Adelabu and Dube, 2015). Alongside this model self-assessment, for the final

515 functional group classes a total of 80 random points were generated across the study site with an equal number in each outputted guild group. These were manually classified using high resolution ortho-imagery from a UAV-RGB (0.02 m resolution) survey from the summer of September 2020, in-field photographs, and study site knowledge. The output classification could was not be seen visible when undertaking this accuracy assessment and the order of the control points shuffled to remove user bias. The classified functional groups classification map produced for 2020 was then used compared to extract the predicted functional

520 groups of these manually classified control points before a confusion matrix was utilised to assess the accuracy of the classification.

3.3. Morphological Change

The M3C2 algorithm (Lague et al., 2013) was employed to calculate morphological change, whereby the surface normals from a subsampled cloud of core points (here at 0.1 m resolution) are calculated, and change along the normal direction is identified with the calculation of a local confidence interval. This overcomes some of the limitations of traditional elevation model differencing which cannot account for the direction of change, ~~a problem that is pronounced for example on the vertical faces of river banks (Leyland et al., 2017).~~ The benefits of using both SfM and UAV-LS data allows their respective drawbacks to be overcome through combining ~~both~~ datasets. SfM has been shown to perform poorly in vegetated reaches where UAV-LS maintains good ground point densities, yet SfM provides good continuity and high point densities in unobstructed areas. Therefore, ~~in order to obtain good ensure the creation of robust~~ surface normals ~~for assessing change~~, both the UAV-LS and UAV-SfM clouds were merged ~~for each survey date~~ (see Tomsett and Leyland (2021) for error analysis) ~~for each survey date~~ and their vegetation removed ~~through the use of the same progressive morphological filter used previously.~~ These resultant clouds were then differenced from their preceding survey date using the M3C2 algorithm.

~~3.4. Assessing Time Varying Eco-Geomorphic Interactions~~

~~In order to identify the presence of any eco-geomorphic feedbacks, and whether there were differences in directions or magnitudes of morphological change between the different functional groups, the classified functional group maps were compared to the morphological change detection datasets. Each pixel of the vegetation maps had the corresponding morphological change values extracted, with the vegetation maps for year one being used for both the February–July 2021 and July–September 2021 morphological change values, and the vegetation maps for year two being used for the September 2021–April 2022 and April–June 2022 morphological change values. The distribution of these datasets as well as the grouped total net change was then compared between each time interval.~~

~~As each of these classification maps utilised data from both summer leaf on and winter leaf off conditions, although they provide a basis for classifying, they do not distinguish between the differing influence that each has on flow. In order to assess this, the point clouds for extracting traits from the herbaceous and tree groups, along with ten individual shrub point clouds, were used to assess the depth varying excess drag created. The depth of interaction was determined based off a peak flood event that occurred in the winter of 2020/21, and although this varies throughout the year, this level indicates the peak interaction between vegetation and flow. The flood extent and depth was modelled using Delft3D, a 2D hydrodynamic model, based on the collected DEMs as well as SfM corrected bathymetry.~~

For each of the functional groups above, the frontal areas at depths of 0.1, 0.5, 1, 2, and 4 m were extracted, with these elevation bands representing natural breaks in different plants vertical structures. Each of these depth dependent frontal areas were then used to determine the excess drag component (F) of a single plant according to;

$$F = \frac{1}{2} C_D A_0 \rho U^2 \quad [1]$$

where C_D is the coefficient of drag, A_0 is the frontal area of the plant facing the flow, ρ is the fluid density, and U is the velocity of the fluid. The U velocity was taken based on the flow speed across the floodplain during the same peak flow event used to estimate flood depth. The excess drag for an individual plant was then transformed in to an excess drag per metre squared using the density obtained for each group in 3.2.2., whereby the number of plants per metre was multiplied by the density. Drag coefficients were estimated using a combination of plant morphology and values from the literature. They were also adjusted seasonally, ranging from 0.6 to 1.2, with foliated plants being subject to a greater reconfiguration process during high flows (Sand-Jensen, 2008; Whittaker et al., 2013). The original frontal areas of each plant were also extracted from defoliated plants, and as such a comparison in the literature of foliated to non-foliated frontal area was used to adjust the frontal areas accordingly at each depth interval (Wilson et al., 2003; Järvelä, 2002b). As a result, four spatial distributions of excess drag were calculated across the domain for the summer and winters of 2020 and 2021 which could then be used to inform how the presence of different vegetation links to its location on the floodplain, and any potential eco-geomorphic feedbacks.

4. Results

4.2. Hydraulically Relevant Trait Analysis

4.2.1. Trait Extraction Error and Analysis of Traits Uncertainty

The QSM analysis appears to output visually sensible results and produce models appropriate for the vegetation being modelled (see Figure 2). The repeat QSM modelling of the individual plants produced consistent trait results. The heights of herbaceous groups were consistent to within 4%, whilst tree groups were consistent to just over 1%. Repeat diameter calculations were within 16% (8 mm 0.08 m) for tree groups and within 18% (2 mm 0.002 m) for herbaceous groups, with higher discrepancies were found in the number of branches. For trees, the number of branches for each model repeat were within 9% of each other, equivalent to 12 branches, whereas for herbaceous guilds functional groups this was 17%, which equates to under 1 branch. The complexity of the larger tree models makes this variation quite likely, especially when the resolution of branches approaches the resolution of the scan data, whereas for herbaceous guilds groups the higher variation is a result of the low number of initial total branches, so an additional branch being identified makes has a larger large impact on

the results. Overall, model repeats of individual plants appear to have good agreement with one another, and provide a basis for separating out vegetation with similar functional traits.

As no in field measurements were taken of plant structure, values When comparing data measured by TLS and UAV-LS (Figure 4A), the UAV-LS performs well, averaging 100.4% +/-1.8% of TLS heights and 103.8% +/-11.2% of TLS DBH values. Discrepancy in the latter may also be influenced by incomplete trunk reconstructions from the TLS scans which did not always capture the full trunk profile. The RMSE in TLS vs UAV-LS DBH was 0.094 m, which is within the same order of magnitude of error identified by Brede et al. (2019). When comparing reconstructed QSM values to those measured directly in CloudCompare, both values for height and DBH align well (Figure 4B). Across all groups, average percentage of reference heights were 100.2% +/- 2.04% and for DBH were 100.2% +/- 10.9%. The greater variation in DBH for herbaceous groups alone (+/-12.01%) is likely due to the stem widths being closer to the precision of the TLS, with any error from manual diameter measurements having a greater impact on comparisons between modelled and referenced data. This suggests that the UAV-LS and QSM methods used reconstruct plant structure well for extracting traits and are suitable for this methodological approach.

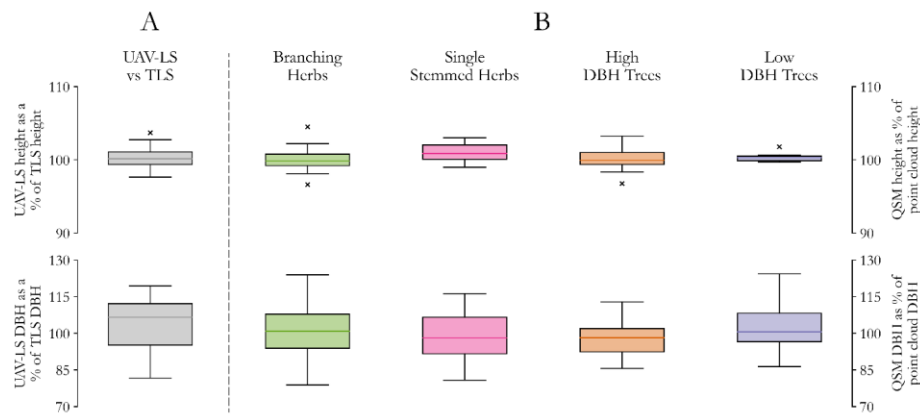


Figure 4 (A) Differences in UAV-LS derived height (top) and DBH (bottom) as a percentage of TLS values for the same trees (n=14), demonstrating good agreement in height and a slight overestimation in DBH from UAV methods. (B) Differences in QSM modelled height (top) and DBH (bottom) as a percentage of measured point cloud data for each of the four functional groups modelled (n=48). Height values are again closely matched with greater variation in DBH values.

Finally, values extracted from the survey data were compared to those found in the wider literature and online databases.

605 Within the tree functional groups, those with a low DBH had an average height of 18.2 m +/- 3.3 m, and a DBH of 0.39 m +/- 0.08 m. Field identification from photos taken on site identified a large number of these trees to be of the Poplar variety. Comparison, and comparisons with both the TRY databases (Kattge et al., 2020) and wider recordings observations in the literature comparing height and DBH for these species showed good agreement (e.g. Burgess et al., 2019; Engindeniz and Olgun, 2003; Zhang et al., 2020) showed good agreement. The range of heights within the TRY database incorporated those measured from the trait extraction methods, and aligned well with the comparison of tree heights and DBH identified by both Burgess et al. (2019) and Engindeniz and Olgun (2003), with the latter studying poplars from Turkey as opposed to the UK. Trees with a higher DBH were predominantly identified as a mix of Willow and Alder, with average heights of 14.9 m +/- 3.2 m and with average DBH values of 0.69 m +/- 0.11 m. This aligned well with the overall height ranges observed in the TRY database for Alder trees, and with the only record with both height and DBH values for Alder showing a tree of 30 m having a 615 DBH of 0.9 m. Southall et al. (2003) found diameters of Southall et al. (2003) found diameters of Willows up to 0.45 m for plants 8-9 m in height, with the trees in this study being both taller and larger in diameter suggesting a difference in maturity. Conversely, both Colbert et al. (2002) and Jurekova et al. (2008) Jurekova et al. (2008) both found DBH values for Willow within the observed range of diameters in this study for trees of similar height. This suggests that although the original QSM methods were tested on Fir, Spruce, Beech, and Oak trees, the methods are suitable for use on a wider variety of trees plants 620 and produce results in line with those expected for the species being observed.

Field observations of the single stemmed herbaceous group identified a dominance of marsh thistle Marsh Thistle, with average heights of 1.14 m +/- 0.17 m and an average stem diameter of 0.013 m +/- 0.002 m. Height values align well with those found in the TRY database, with the majority of recorded heights between 0.8 – 2 m (Kattge et al., 2020). Van Leeuwen (1983) Van 625 Leeuwen (1983) measured stem circumferences of between 26-70 mm 0.026-0.070 m, equating to diameters of between 0.008 and 0.022 m, yet very little other literature or values on stem circumference or diameter are available. Never the less, both the observations of height and thistle stem diameters suggests that the modelling has effectively reconstructed the vegetation. Likewise, comparison between the average height values of the branching herbaceous group, predominantly identified as hedge 630 mustard Hedge Mustard, and those values in the TRY database indicate good agreement, with reconstructed values from the field having heights of 0.46 m +/- 0.12 m and values in the TRY database averaging 0.49 m, albeit with a much higher variation of +/- 0.25 m. As with the single stemmed herbaceous group, there is very little data to compare obtained values of stem diameter with. It would be expected that the branching herbs would have a lower diameter based on field images, and this is the case with an average of 0.011 m +/- 0.003 m. However, this is approaching the likely limit of detection of the TLS scans, whereby the stem diameter approaches the resolution of the scan data. Yet for both of the herbaceous guilds, the methods 635 deployed appear to have consistently modelled individual plants, and produced values in line with those in the wider literature. For both the herbaceous and tree groups, the extracted traits can be reliably used to examine which traits distinguish between different functional groups.

640 Overall, this methodological approach has provided a good basis from which to extract traits. Both UAV-LS and TLS have proved effective in modelling various vegetation, and the QSM analysis has produced models that match well to the original point clouds. Likewise, the values extracted for the species identified in the field match well with those in the wider literature and online databases. Overall, this provides some confidence in the methods used to separate functional groups and scale these to reach based metrics.

4.2.2. Functional Group Results

645 Figure 65 shows the PCA plots of ~~(A)~~ herbaceous vegetation metrics from the TLS scans; ~~(A)~~ and ~~(B)~~ woody vegetation metrics from the UAV-LS scans; ~~(B)~~. It is clear that some separation of points through dominant metrics is possible, with both plots exhibiting two principal components capable of separating the defined functional groups. ~~Panel A shows the PCA plot for~~ herbaceous vegetation. ~~Height (Figure 5A), height~~ is identified as a clear principal component between each ~~and~~ functional group, as well as volume. Although the number of branches was not a key component for separating functional groups, branches per unit height explained some of the variability in the data. Taller plants may have a similar number of branches, and so accounting for plant height produces a density of branches independent of size to help explain plant structure. Of the four identified components, only ~~the~~ height is identifiable from the UAV-LS data for upscaling, however, point density and spectral properties may improve group separation. ~~Panel B shows the PCA plot for~~ woody vegetation. ~~Height (Figure 5B) height~~ is less important in distinguishing the two functional groups than for herbaceous vegetation, yet trees under or over certain heights are likely to be one group or the other suggesting minimum and maximum threshold values. For separating functional groups, the most important components appear to be DBH and vertical skew which was expected as this was the basis for initial functional group classes. DBH cannot always be easily extracted from UAV-LS data if it is incomplete, therefore as the vertical distribution acts in the same component direction, this can be used as a potential ~~method~~ metric for differentiating functional groups. There is however considerable overlap in both of these PCA plots for woody and herbaceous vegetation. There are dominant trends such as the DBH and plant height for separation, but there is considerable variation within the functional groups for their QSM based metrics which may impact the final classification.

650

655

660

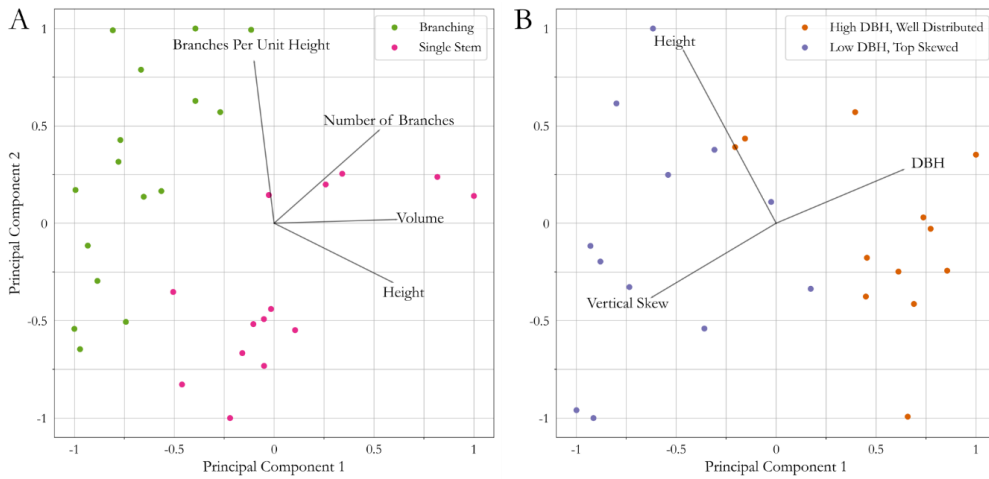


Figure 65 PCA analysis of (A) herbaceous branching and single stemmed vegetation and (B) high DBH and low DBH tree functional groups to investigate differences in trait characteristics. Lines indicate the direction of each variable that explains variation in the data.

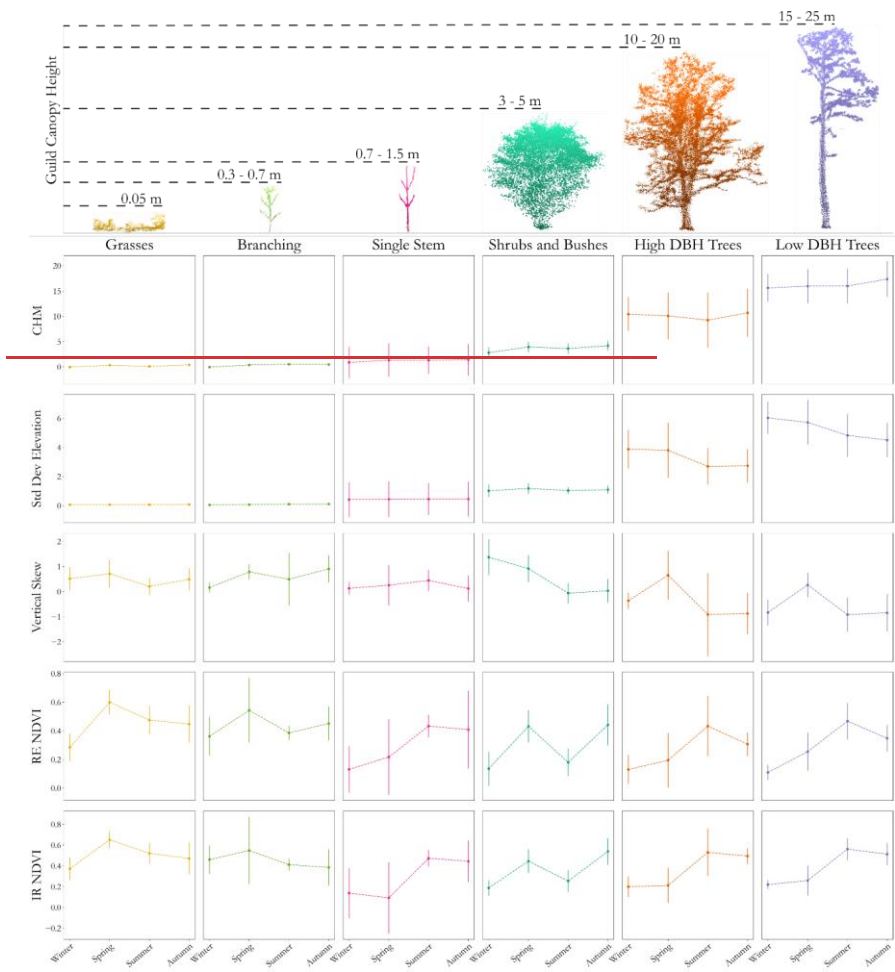
4.2.2. 4.2.3. Linking PCA Clusters to Reach Scale UAV-LS Data

Figure 76 shows the results of the seasonal analysis of different variables derived from UAV-LS and UAV-MS imagery for each of the functional group classes. There are clear variables which can separate different functional groups with ease, for example the height of the canopy is a key indicator between woody, herbaceous, shrub, and grass functional groups. Separating out similar functional groups does appear to be more nuanced. The High DBH and Low DBH woody functional groups both have very similar values and seasonal patterns of changes in NDVI values as well as in their height. This is unsurprising as the PCA analysis showed, with height not being a dominant factor in explaining variation, with numerous samples showing crossover. Vertical skew did show group separation, with the samples used for QSM analysis collected in leaf-off conditions. Figure 7 does suggest suggests that changes in winter skew are visible between the two tree functional groups, with a smaller amount of crossover as expected. Spring, summer, and autumn Summer skewness is less informative, likely due to leaf-on conditions effecting affecting full tree reconstruction, with higher variability in results between the sample areas. For example, a tree that has little understory reconstructed is likely to show little vertical skew, compared to one where below canopy data is collected.

Formatted: No bullets or numbering

Separating out herbaceous functional groups is also a challenge. CHM values for single stemmed herbs are more variable and cross over ~~in to~~ into grasses and multi-branching herbs. However, the mean CHM values are higher, in line with the PCA analysis, and may enable herbaceous group separation. Likewise, the average skew values help to differentiate between classes, but again the variability in the data suggests it is harder to separate by structural content alone. Conversely, spectral data shows great promise in differentiating between functional groups. Both the absolute values between herbaceous functional groups show different as well as their seasonal patterns especially when utilising the red edge band for NDVI calculations.

685



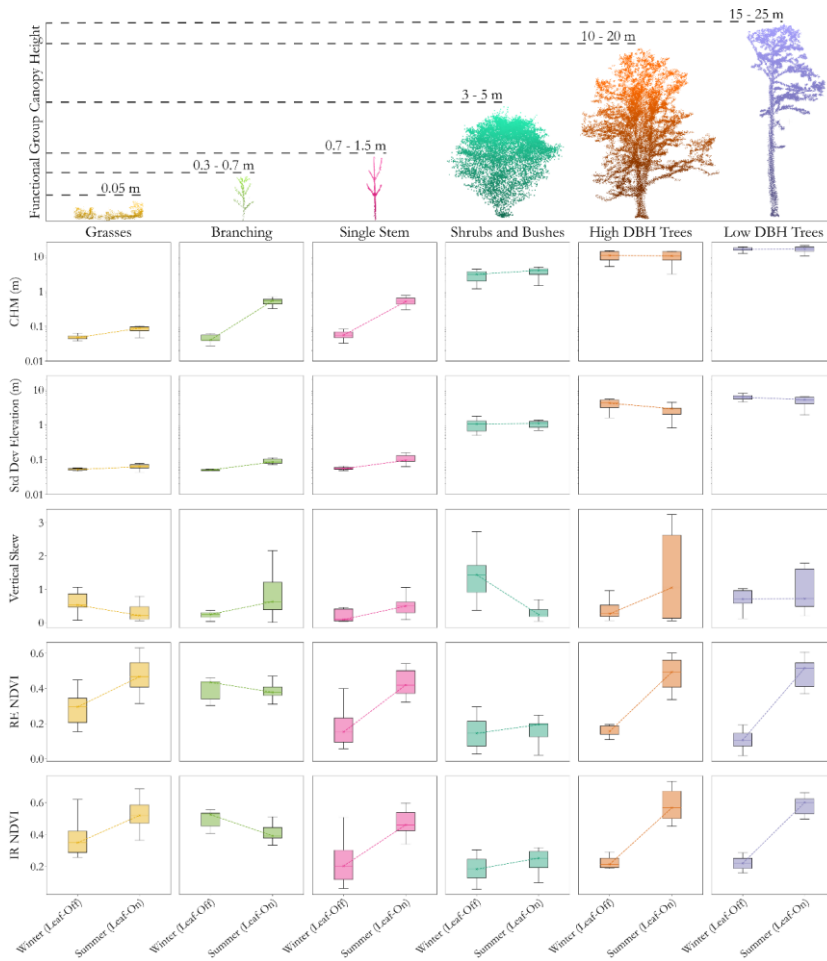


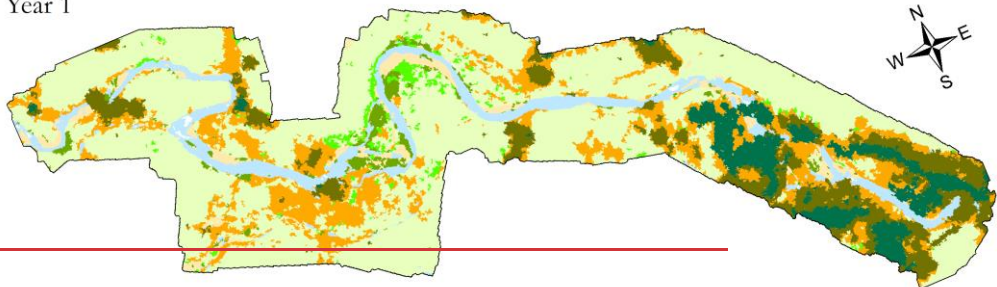
Figure 76 Results of seasonal leaf-on/leaf-off analysis (X-axis within subplots) of different reach scale metrics (Y-axis) from UAV-LS and UAV-MS data for each identified guild-plant functional group. The point clouds at the top provide an example of vegetation in each functional group, with canopy height ranges acquired from trait extraction for the four analysed functional groups and from the reach scale analysis for the remaining grass and shrub functional groups. Error bars Box plots indicate one standard deviation around the mean, distribution of values derived from the reach scale data for individual plants. CHM (Canopy Height Model) is given in metres and is plotted in log scale to show the variation for shorter functional groups. IR refers to Infra-Red and RE to Red-Edge bands in the NDVI calculations. Winter data is from February 2020, and summer data is from July 2020. For plants in the tree groups from the half of the reach not surveyed in July, data from September 2020 was used.

4.2.3. 4.2.4. Creation of Seasonal Reach Scale Functional Group Maps

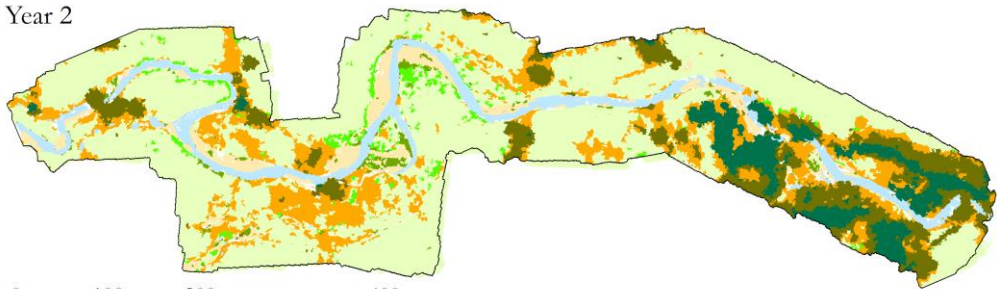
700 The annualised reach scale ~~classification-classifications~~ (combinations of winter and summer data) based on functional groups
and land cover is shown in Figure 8. ~~There appears to be an over-classification of branching shrubs based on initial comparisons
with ortho-imagery, where the edges~~7. Areas surrounding both high and low DBH tree groups show a prominence of larger
vegetation ~~and some predominantly grass regions appear to have been misclassified shrub groups~~. This may be due to
segmented regions during the image classification at the large variation in structural and spectral characteristics ~~edge~~ of this
705 trees having heights similar to those of the shrubs group ~~which were less well accounted for,~~ possibly leading to a false
classification not picked up in the accuracy assessment against the manual classification. Herbaceous groups were predicted
in areas ~~that were expected,~~
typically associated with such vegetation; being close to the channel, in paleo-channels which are reactivated over winter, and
in mobile areas of the ~~channel were~~ reach where larger vegetation would find it more challenging to establish. The out-of-bag
710 accuracy score when training the random forest classifier with 300 trees was 87.2%. Figure 9-A8A shows the importance of
each band in the classifier, with structural elements proving key in separating functional groups, especially using summer
standard deviation

Formatted: No bullets or numbering

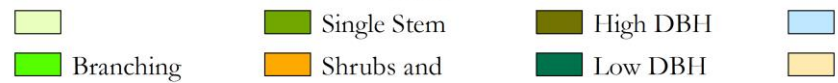
Year 1



Year 2



0 100 200 400 Metres



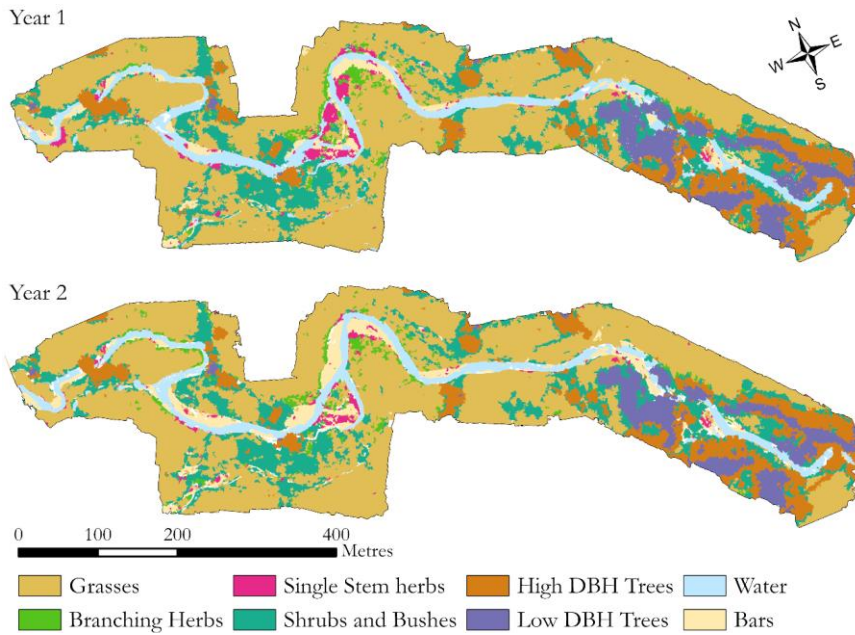
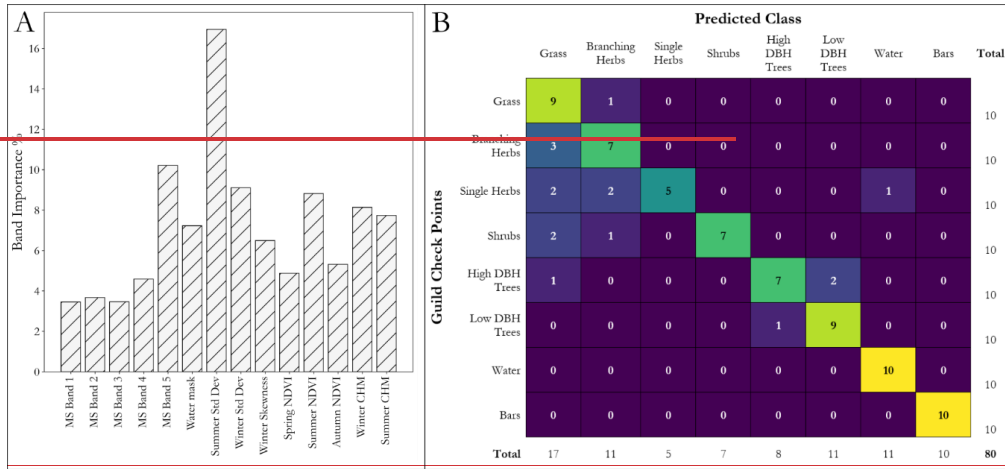


Figure 87 Resulting classification from reach scale analysis for the areas covered by both UAV-LS and UAV-MS data for year 1 and year 2 of the surveys. Note the over-classification of shrubs and bushes, especially at the edge of larger wooded groups, and the changes in channel planform and functional groups through the central section of the reach compared to the relative stability at each end of the reach.

of point heights. The near infra-red band and winter standard deviation are the next most important elements, with the remaining individual spectral bands providing a smaller contribution to the classification. The higher importance of the two NDVI layers implies that providing the classifier with analysed image data is more useful than individual bands alone. Likewise, the canopy models alone are less informative than the variation in plant height when detecting functional groups, supporting the use of manipulated rather than simple metrics to help improve classification.

The accuracy assessment confusion matrix can be seen in Figure 9-B8B, comparing the number of manual check points that are correctly and incorrectly predicted by the classifier. The overall model accuracy is 80%, lower than the out-of-bag prediction. However, this is not surprising as training areas were delineated based on complete structural profiles for the QSM analysis and the total number of samples used for training was small relative to the possible variation across the reach. There was a general over classification of points as within the grass functional group, with only one grass control point

incorrectly classified as branching herbs. Branching herbs which are more detectable from imagery and likely to return more laser scan points were classified reasonably well, only being misclassified as grass.



735

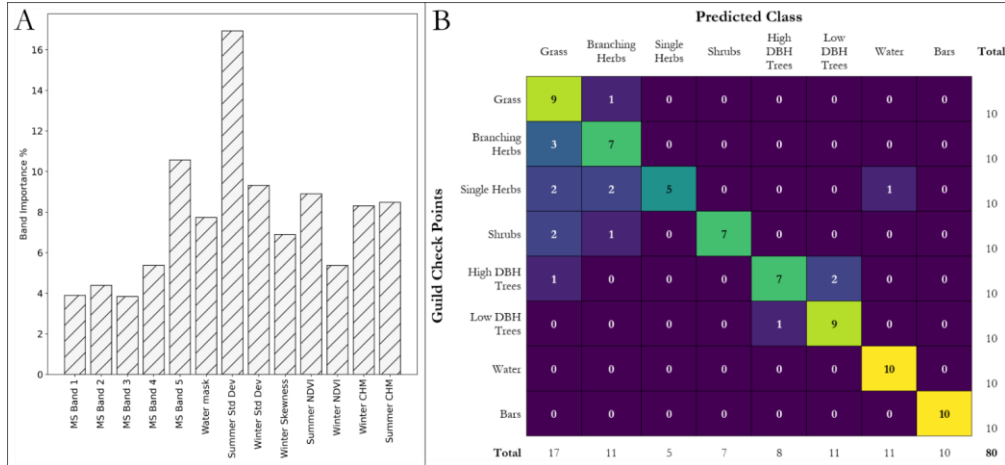


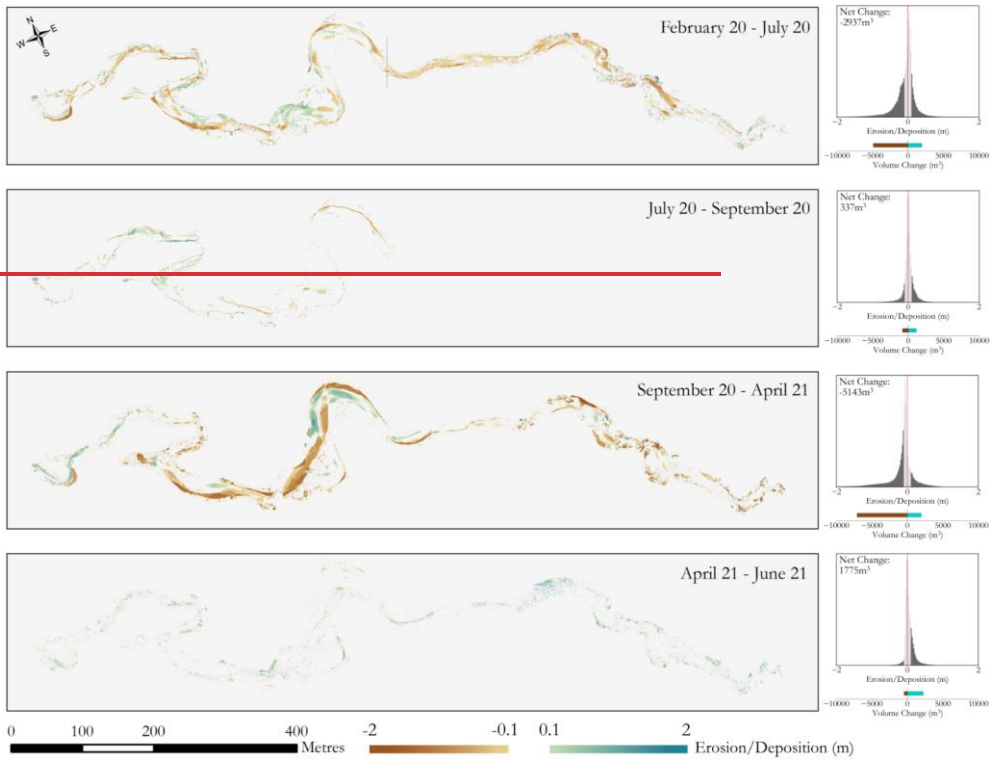
Figure 98 Individual band importance in the final classification (A) and confusion matrix (B) from the accuracy assessment. The band importance represents the contribution of an individual layer to the final classification. The confusion matrix demonstrates for which functional groups the classification struggled, showing an over-classification of grasses and the poor detection of single stem herbs. The overall classification accuracy was 80%.

740

Single ~~branchingstemmed~~ herbs ~~however~~ were relatively poorly classified (50% accuracy), being misclassified as grass, branching herbs, and even water. However, their narrow structure and sparse spacing make them hard to identify from coarser imagery and ~~they return fewer laser scan points-UAV-LS~~. This class also exhibited ~~the greatest variation~~ large variations in values when using reach scale metrics to evaluate functional group samples. ~~overlapping with several other classes~~. Shrubs were predominantly misclassified as branching herbs and grass; this may be due to the object segmentation not always isolating complete plants or including surrounding ground points which may have affected the classification. Low DBH trees with a top skew were classified well by the model, most likely due to their larger heights and winter skew, whereas higher DBH trees were misclassified as both low DBH trees and grass. The former likely due to the difficulty in separating out these two functional groups which have subtle differences in certain classification layers such as winter skew, and the latter from surrounding data being included in ~~ana segmented~~ object ~~likely~~ from factors such as shadowing continuing an object outside its true bounds. However, of all 20 tree check points, only one was incorrectly classified as a functional group with clearly different traits, a High DBH Tree ~~segment~~ as Grass (see Figure 98B).

4.3.4.2. Morphological Change

As ~~is~~ expected, the majority of morphological change occurs over winter months (Figure 9) when there are ~~high~~ higher flows (Figure 10). Conversely, over periods of lower flow (see Figure 1) during the summer both the extent and magnitude of change is reduced. Throughout the first winter period erosion occurs on the outer bank edges with fairly consistent planform evolution throughout the reach. Deposition is evident throughout the entire reach, however erosion is considerably more dominant than deposition, with just under 3000 m³ of net erosion. The second winter appears to have more localised effects on morphology, with clear channel reshaping through the upper half of the study area. Overall, despite having similar levels of deposition across both winters (~2000 m³); ~~the~~ increase in erosion for the second year ~~possibly due to an increased level of time at higher flows~~ has led to a greater increase in net erosion (~~~7000~~ 5000 m³). Both histograms of change within the winter seasons show a dominance in erosion overall. Over both winters, morphological change in the tree group dominated downstream reach has undergone similar levels of change with areas ~~of~~ erosion and deposition influenced by the presence of large vegetation. Both summer periods have a greater degree of stability, with erosion and deposition taking place but in lower magnitudes. This is consistent throughout the reach with no hotspot areas of either deposition or erosion, with deposition showing to be more dominant overall.



770

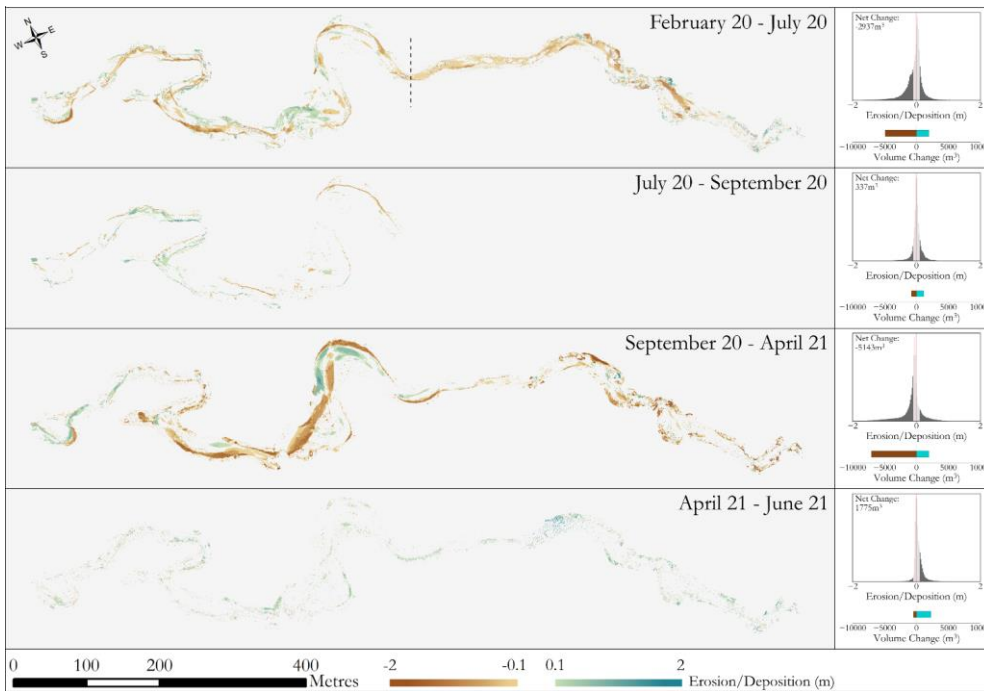
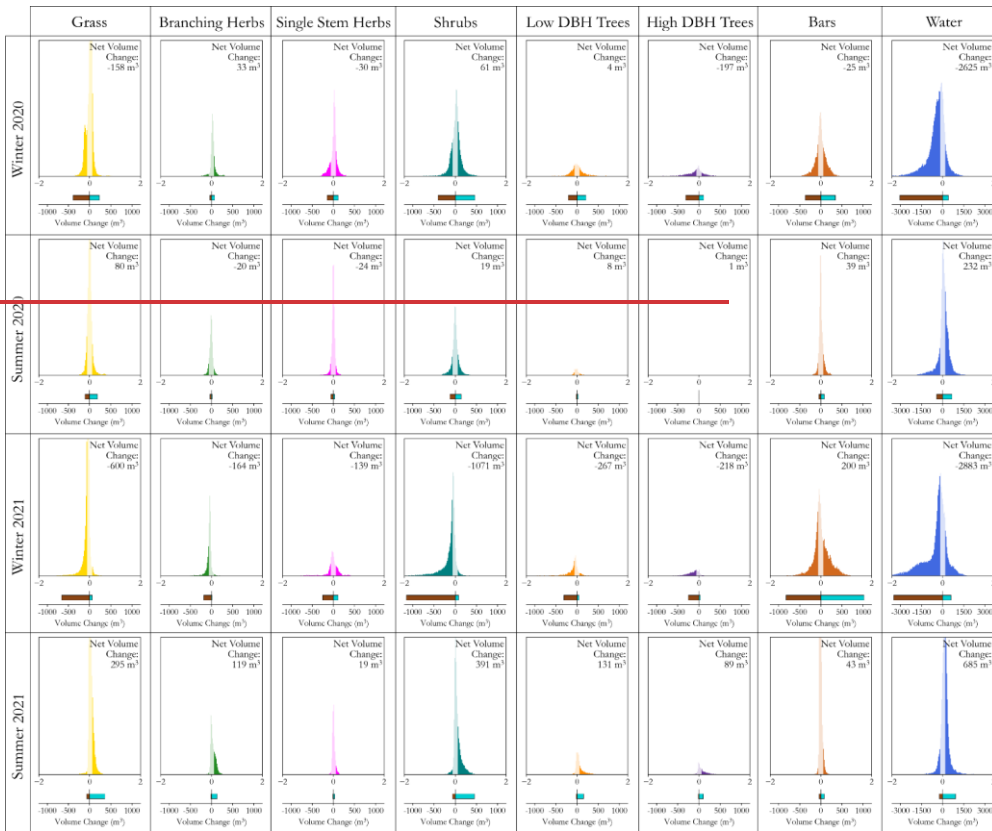


Figure 409. Morphological change throughout the monitoring period, showing the spatial variation in erosion and deposition as well as the net change in sediment. Note that February 20 – July 2020 is a composite DEM of difference consisting of comparisons between February and July to the left of the dashed line and February to September to the right of it. In July, only half of the survey area was captured. The stability of the reach over summer (July to September) justifies attributing change to the February – July result. Change less than 0.1 m in elevation was not shown as this was deemed below the level of detection of the sensor (see Tomsett and Leyland (2021) for accuracy assessment details). The histograms adjacent to each time period show the distribution of magnitude of change, the volume of erosion and deposition over that time period, and states the net volume change across the corresponding time periods. Areas of the histogram in light grey depict change below the 0.1 m level of detection.

4.4.4.3. Eco-Geomorphic Interactions

A key benefit of being able to identify the location of different functional groups, is the ability to decompose the overall distribution of morphological change in-to each functional group for each time period (Figure XFigure 10). When assessing the distributions of erosion and deposition between groups across the four time periods, each functional group follows the overall pattern presented in the general morphological analysis, whereby there

is a clear dominance of erosion over deposition ~~signals~~ in winter, and a balanced or deposition dominant signal in the summer periods. ~~Unsurprisingly, there is a dominance~~ Unsurprisingly, erosion dominates in both winters ~~of erosion in~~ for locations that are classed as water due to lateral migration of the multiple areas undergoing switches in channel location in this time. In this case the presence of ~~planform~~ planform change was the prominent form of morphological change, accounting for a large proportion of the net volume shift, with only grass and high DBH trees seeing large volumes of net erosion at over 100 m³. In fact, when compared to the changes in the summer, most of the functional ~~grups~~ groups saw similar magnitudes of change across the two time periods. Compared to winter ~~2021~~ 2021 however, the net change in volume for areas classified as water was similar, with the ~~remainder~~ remainder of change ~~happening~~ happening throughout the remaining functional groups and on ~~exposed~~ exposed bars. During this time, there was net deposition on channel bars, however there are large ~~quantities~~ quantities of both erosion and ~~deposition~~ deposition in this group, in line with the highly active nature of such features. Whilst across all functional groups there is an increase in the net erosion compared with the first winter period, this is ~~exaggerated among~~ exaggerated among grasses and shrubs, accounting for 32% of net erosion. For both cases, these are likely to be the result of channel reactivation during overbank flow removing ~~large quantities of~~ large quantities of floodplain sediment. Throughout all of the time periods, no group ~~has seen~~ exhibits a ~~consitent~~ consistent pattern of erosion or deposition, changing based on season and year, making it difficult to identify any direct eco-geomorphic ~~feedbacks that are present~~ interactions at these scales over these two winter periods. However all groups appear ~~to~~ to undergo a ~~dominant~~ dominant erosion signal in the winter followed by an ~~accretion~~ accretion signal in the summer, ~~possibly~~ possibly suggesting that vegetation that can recover or survive ~~winter~~ winter peak flows ~~goes on~~ goes on to trap sediment and stabilise the channel and adjacent floodplain.



805

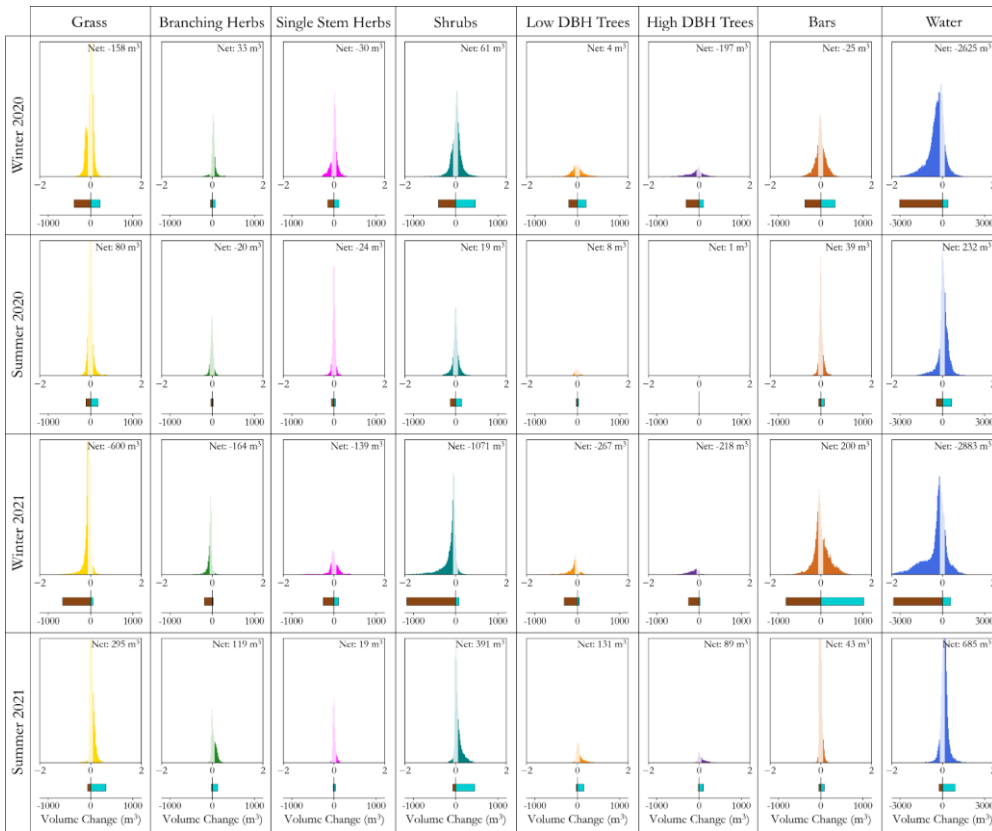


Figure X.10. Histograms of morphological change for each classified functional group (X-axis) location throughout the reach for each of the time periods studied. (Y-axis). Below each is the volume of erosion and deposition in m³, as well as the net volume change stated in the upper right corners. The transparent elements of the histogram show the change that occurred below the minimum level of detection, and was not included in the erosion, deposition, and net volume change information. Note the change in X axis values for the erosion and deposition bars for the water class so as not to subdue the other groups due to the disproportionate amount of change over both winters here.

810

815

Importantly, the above results show the spatial relationship between different functional groups and the geomorphic change that occurs at that location. Yet, the interaction each group has with flow is not accounted for, with different groups having a different proximity to the channel and areas of overbank flow. To assess the influence that each functional group is having on

820 flow, the spatially-varying drag calculated in section X.X. was aggregated to identify how different guilds affected drag through the reach across each time period. Table X documents the change in both the area of each guild between each year, and the various excess drag provided across the domain between summer and winter and between each year. Overall, it is clear that shrubs have the greatest influence on flow in terms of excess drag, due to their density and the consistently vegetated vertical profile. Low DBH trees also have relatively high excess drag across the reach, and when compared to the high DBH trees will exert a large influence on flow through the catchment. This is again most likely as a result of density, as the frontal area of the low DBH trees will be less than those with a higher DBH, but the measured density of low DBH trees is an order of magnitude less, and as such has less influence on overland flow. The excess drag created by single-stemmed herbs in comparison is similar to that of high DBH trees, implying that proximity to the channel, group coverage, depth of flow interaction, and seasonality, can all influence which functional groups play the biggest role across the domain.

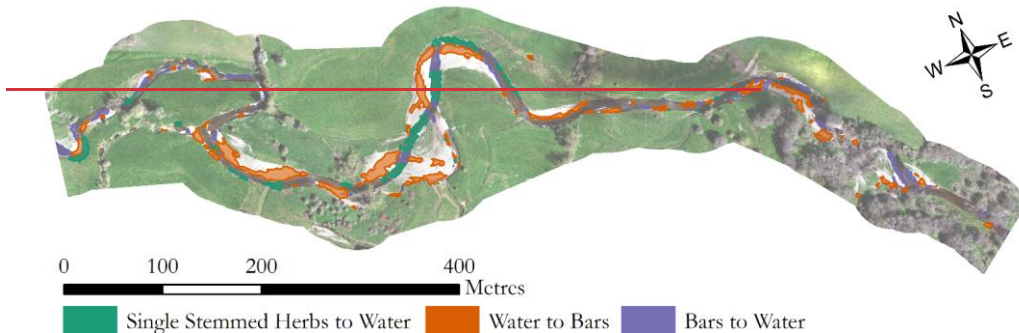
830 The largest changes in excess drag between summer and winter drag occur within the herbaceous and shrub groups, with single-stemmed herbs observing the largest increase in excess drag. Unsurprisingly, as the majority of interaction between trees and and flow remains consistent throughout the year, these experience the smallest difference in excess drag. These increases in excess drag may provide an explanation of the deposition occurring in the summer months; and despite the lower flow depths occurring in the summer the increased foliage will help to trap any sediment during higher flow events.

855 **Table X. A comparison of total excess drag calculations for the functional groups across the study site, comparing changes both between seasons and years, as well as assessing changes in group extent between both years. Changes in seasonal drag are between the summer of year 1, and the winter of year 1, whereas the changes in annual drag are an average of the changes between winter year 2 and year 1, and summer of year 2 and year 1. No excess drag was calculated for grass, water and bars, and so only comparisons in spatial extent are examined for these groups herein.**

	Year 1				Year 2				
	Area (m ²)	Excess Drag (N)		Seasonal Change in Drag	Area (m ²)	Annual Change in Area	Drag (N)		Annual Change in Drag
		Winter	Summer				Winter	Summer	
Grass	49358	-	-	-	49671	1%	-	-	-
Branching Herbs	2564	19	21	10%	2784	9%	22	24	12%
Single Stemmed Herbs	3388	76	100	31%	1680	-50%	38	49	-49%
Shrubs	20240	511	614	20%	18780	-7%	439	527	-14%
High-DBH Trees	8956	33	35	7%	8744	-2%	34	37	4%
Low-DBH Trees	5960	135	144	6%	5732	-4%	120	127	-12%
Water	12360	-	-	-	11218	-9%	-	-	-
Bars	4981	-	-	-	7872	58%	-	-	-
Total	107807	775	914	18%	106481	-1%	652	765	-16%

860 When comparing the annual changes, there are large shifts in both the drag components of individual groups and overall excess drag throughout the reach. Changes in drag can be attributed to total cover of each functional group, such as branching herbs where both area and drag increase by similar proportions, and the small decrease in High-DBH trees is accompanied by a small increase in drag. Yet, for both low-DBH trees and shrubs, the separation between the two suggests that the distribution of each group is changing so that the interaction with flow is less. The drop in both area and subsequent drag from single-stemmed herbs at first seems to be related to the increase in area of channel bars, suggesting a removal of such vegetation in situ. However, as figure X shows, the change that is most prominent is from single-stemmed herbs to water, whereby the channel has removed vegetation, and bars have formed in place of the old channel which are yet to be established with vegetation.

865



870 **Figure X.** The three most common changes in functional groups across the study site, accounting for 45% of all change. Water to bars was the most common change (28%), followed by single stemmed herbs to water (9%), and then bars to water (8%).

5. DISCUSSION

5.1. Trait Extraction and Functional Group Formation

875 Current measurements of plant functional traits are still predominantly ground based and therefore limited by on site access (Palmquist et al., 2019), requiring extensive sampling to extract enough data to create functional groups relevant to a particular study (e.g. Diehl et al., 2017a; Hortobágyi et al., 2017; Stromberg and Merritt, 2016) and require extensive sampling (Palmquist et al., 2019; e.g. Diehl et al., 2017a; Hortobágyi et al., 2017; Stromberg and Merritt, 2016). Remote sensing of these traits is therefore a potentially novel/useful way to collect data across large/larger areas, depending on the vegetation size and methods of data collection. Although no ground truth data relating to traits was collected in the field, the assessment of variability in model construction, comparisons between TLS and comparison UAV-LS data, UAV-LS data and reconstructed models, and reference to wider records based on dominant species in databases and the literature suggests that the method performed well at extracting methods developed herein were reasonably able to extract physical attributes. This highlights the potential of remote sensing to collect structural trait data for eco-geomorphic research moving forward, especially once trade-offs in terms of time and spatial extent are accounted for. For example, data from field surveys are generally limited to that site, and although the findings can be applied to locations elsewhere, this requires knowledge of the vegetation present at this site. Yet, if these can be extracted from remote sensing and have a classification analysis run across them, this represents an improvement in the applicability of traits based research.

880

885

The use of pre-determined rather than site specific functional groups was a method employed by Butterfield et al. (2020) on the basis of those outlined in Diehl et al. (2017a). The sites used/vegetation in both of these studies were/was similar, and the

890

application to a temperate UK based site is challenging. ~~However, because of the lack of a comprehensive list of functional groups for riparian vegetation made using predetermined guilds justified complexity and similarities of some plants.~~ When compared to previous studies, the reduction in the number of ~~analysed herbaceous guilds~~ functional groups used herein is due to the data resolution, whereby only two categories could be ~~distinctly observed and extracted.~~ Yet, for woody species, the method allowed for separation of two sub-classes which have different impacts on flow, especially when used to determine ~~excess drag explicitly detected.~~ The methods used provided ~~sensible~~ use of a PCA led to the ~~successful~~ separation of functional groups, each of which have a different hydraulic highlighting metrics which could be used to separate them over larger scales. ~~The influence. Single-stemmed herbs were taller and although the number of branches was similar to the branching- that different herbaceous group, the number of branches per unit height was lower. A taller, stronger, vegetation, with variable flexibility and less-branching herb structure, has on flow is going to have a distinctly different impact than a shorter more flexible one well studied (e.g. Nepf and Vivoni, 2000; Järvelä, 2004; Sand-Jensen, 2008), and being able to differentiate successfully between these two groups highlights the success applicability of the survey and trait extraction methods developed in this research.~~ Likewise, the difference in flow conditions between low DBH trees that are closely packed to less densely packed high DBH trees may show a resemblance to the influence found at smaller scales on plant density (Järvelä, ~~2002b~~ 2002a; Kim and Stoesser, 2011); ~~with noticeable differences in subsequent excess drag values.~~ The relationship between DBH and vertical skew is not surprising; ~~considering the higher plant spacing density the competition for space is likely higher, resulting in more mass higher up the tree profile. As, and as plants cannot yet could not be easily differentiated by measuring their DBH, using vertical skew gives/provides promising results for upscaling to larger areas whereby ALS surveys may be able to differentiate between woody functional groups for better informed hydrological analysis,~~ with similar work being done using vertical distribution to classify forests already (Antonarakis et al., 2008; Michałowska and Rapiński, 2021).

~~However, UAV-LS data for QSM has been shown to overestimate canopy reconstruction volume (Brede et al., 2019; Dalla Corte et al., 2022), which mirrors the over complexity demonstrated in Figure 2 (QSM Cylinder Model) with some awkwardly orientated cylinders. Extracting traits using remote sensing is novel and can outcompete ground-based methods for coverage but is not yet likely to match the accuracy and interpretive ability of in-field measurements, as shown in estimations of forestry structure for height, DBH, and volume (Dalla Corte et al., 2022). Moreover, the use of TLS for analysing herbaceous guilds/the QSM Cylinder Models (Figure 3). Extracting traits using remote sensing can improve on ground-based methods for coverage but cannot match the accuracy and interpretive ability of manual in-field measurements yet, as shown by Dalla Corte et al. (2022) for height, DBH, and volume. Moreover, the use of TLS for analysing herbaceous functional groups is highly localised (Lague, 2020), meaning only a small number of samples can be analysed which may not reflect the full variation in vegetation morphology. The UAV-LS data, although covering more ground, does take significant levels of time to post-process and extract multiple individual vegetation models, although as the spatial extent of coverage increases, the time gains improve as the same vegetation models can be used to classify increasingly larger sites. Algorithms which can extract traits and classify large areas are likely to improve in much the same way that SfM methods developed, such as those presented by Burt et al.~~

925 (2019) and Krisanski et al. (2021). The UAV-LS data collected for this study took a significant amount of time to post-process,
in the region of days for each survey and weeks for the remaining analysis. Yet, algorithms which can extract vegetation and
classify large areas are improving in much the same way that SfM methods have developed, making processing times quicker
and allowing for a greater number of plants to be analysed (e.g. Burt et al., 2019; Krisanski et al., 2021; Yarroudh, 2023; Letard
et al., 2023).

930 Currently, UAV remote sensing methods can only obtain above ground structural traits, and although these make up a
significant component of hydraulically relevant traits, they do eliminate the collection of traits such as root structure, strength,
and plant flexibility. Both UAV-LS and TLS also struggle to capture the complex structures of shrubs, with TLS requiring too
many scans to resolve the structure of enough samples (Boothroyd et al., 2016; Olsoy et al., 2014) and UAV-LS having too
935 low a point density and canopy penetration for such complex branching. However, methods pioneered by Manners et al. (2013)
may help to overcome this by relating vertical profiles from TLS and ALS data to enable upscaling to larger extents. Similar
approaches may help to overcome this. Similarly, more work is needed to overcome the difficulty in separating out species
that appear similar structurally and spectrally alike, such as woody saplings and herbaceous plants, but that will perform a very
which may have different role when interacting hydraulic impacts. At present, these two different vegetation types could easily
940 be misclassified, and with the likely different interactions with flow. In this study, such differences have not been accounted
for, but presents a future area of work to establish the implications and subsequent morphology, not being able to account for
these with remote sensing is a limitation. Efforts to further investigate this, possibly using proximity measures to other
functional groups, or probabilistic rather than categorical classification methods, may help to overcome the issue.

5.2. Reach Scale Guild mapping Functional Group Mapping

945 The benefits of remote sensing of plant traits does not come become evident when scaling from individual plant to reach scale
analysis but from upscaling to larger extents. Using the same datasets provides continuity between both the individual analysis
and reach wide guilds. Finding common features of defined guilds functional groups is more computationally effective than
analysing every individual plants plant throughout the reach at present. Using structural characteristics of the point cloud
alongside spectral properties across time allows the temporal leaf on/leaf off patterns to enhance guild functional group
950 classification. It is clear that distinctive initial separation between guild functional group types can initially be made based on
canopy height, although this presents a challenge at the transition between groups. The need for seasonal data is emphasised
across functional groups, whereby herbaceous, Herbaceous groups benefit from having winter and spring seasonal patterns in
NDVI values to complement the difference variation in height, and tree groups require leaf off vertical distribution to help with
separation, supporting previous work emphasising the need for seasonal data to improve eco-geomorphic research
955 (Nallaperuma and Asaeda, 2020; Bertoldi et al., 2011). Overall, with single stemmed herbs appear appearing to be more show
greater seasonal, with lower winter values than branching herbs, whereas shrubs NDVI experience a dip in spring surveys as
a consequence of flowering affecting spectral properties. For tree groups, capturing data later in the year has a greater overlap

960 variation. Tree groups however require leaf-off data to improve canopy penetration to help separate out each functional group, and as such the timing of data collection will likely impact ~~classification results, with some guilds being better separated at different times of the year.~~ For the effectiveness of this method. Previous work has emphasised the need for seasonal data to improve eco-geomorphic research (Bertoldi et al., 2011; Nallaperuma and Asaeda, 2020), which the results of our research support. Moreover, for these methods to be applied elsewhere, it therefore follows that the seasonal monitoring implemented at other sites a seasonal approach used herein and in other studies (Van Iersel et al., 2018; Souza and Hooke, 2021) to surveying is required:

965 ~~The use of random forest classification for this study site, as has been successful and builds on the growing body of research for their application to high resolution classifications undertaken in similar studies (Adelabu and Dube, 2015; Chan and Paelinckx, 2008; Adam and Mutanga, 2009)(Van Iersel et al., 2018; Souza and Hooke, 2021), yet this present a limitation for some research.~~

970 The ~~misclassification accuracy~~ from the random forest classifier ~~are~~ is in line with ~~misclassification experienced those reported~~ by Butterfield et al. (2020) ~~when using who used~~ multispectral imagery alone, with most misclassifications happening in ~~guilds adjacent and most functional groups which are similar to the true class.~~ This is unsurprising when ~~the~~ viewing the uncertainties in functional group properties in (Figure 7.6), where there is evidence of overlap across multiple attributes for two different groups. Moreover, where there are transitions between guilds with ~~Therefore, adjacent groups may be erroneously classified due to having similar properties, or where the spectral and structural characteristics, as well as image segmentation has incorrectly defined 'similar' pixels, it is likely that misclassification may occur including two groups within one segment.~~ Identifying ways to better segment regions of vegetation may help to improve the overall classification success. ~~A related drawback is the categorical output used in this method, that a segmented region must be one type of functional group, and a such cannot distinguish between the presence of multiple groups. This is especially the case for woody regions, who will have a mixture of.~~ However, the outputs here add to the growing body of research using random forests for high resolution classification approaches (Adelabu and Dube, 2015; Chan and Paelinckx, 2008; Adam and Mutanga, 2009). As the methods here only assign one group for each image segment, elements such as understory vegetation ~~which is not characterised, and is another area which may need further work to account for the hydraulic, which will influence this has overbank flow, are currently not accounted for.~~

990 Despite ~~the above these~~ limitations, the resulting classification accuracy (Figure 8.7 and Figure 9B8B) shows promise for linking local scale trait modelling to larger scale functional group mapping. The overall spatial distribution of classes throughout the reach is as expected aligns with the wider literature, with herbaceous species dominating the active meandering section as these are more adaptable to changing topography and flood conditions, whilst larger woody species are seen in more stable sections of the river as these species which require more stable hydraulic conditions are seen in less active sections of

995 ~~the reach~~ (Kyle and Leishman, 2009; Stromberg and Merritt, 2016; Aguiar et al., 2018). The classification ~~herein takes a~~
~~different approach to work by~~ (Butterfield et al., 2020) ~~who used imagery to classify species and subsequently assign~~
~~vegetation groups, whereas the remote sensing method used here utilises the methods herein utilised a mix of structural and~~
1000 spectral ~~characteristics data~~ to ~~designate the spatial~~ determine functional group distribution ~~of functional groups, removing, as~~
~~opposed to~~ the species identification ~~component and subsequent grouping performed by Butterfield et al. (2020)~~. This is
important as the same species may display varying traits-based on their proximity to the channel (Hortobágyi et al., 2017) ~~and~~
~~as such,~~ (Hortobágyi et al., 2017), ~~and as such~~ using the physical characteristics of plants can be seen as an advantage. ~~Species,~~
yet species identification still plays an important role, ~~and has been used in this study to both assess the reconstruction of~~
1005 ~~vegetation and to inform the coefficient of drag values used. However, as noted previously. However,~~ obtaining secondary
data on ~~a range of plant species~~ traits that are relevant to the area of study can be challenging, (see 4.2.1.), and may limit the
applicability of traits-based methods ~~into~~ the wider scientific community.

5.3. Eco-Geomorphic Change

1010 ~~Given the hydrology of the river, the majority of morphological change occurs over the winter months as expected. Yet the~~
~~temporal resolution of the surveys is not capable of picking out whether this is the result of a single flow event or continuously~~
~~high flows.~~ There appears to be more localised evolution in the second winter of surveying whereas the first winter appears to
show ~~a more~~ ~~continual~~ consistent response throughout the reach. The singular lower peak in water levels for the second winter
as opposed to several higher peaks in the first (see Figure 4.1C) suggests that priming may be more important for ~~large~~
~~avulsions~~ channel movement, whereby a ~~singular~~ single flow event of lower magnitude can incite a greater resultant planform
1015 shift. ~~However, without multiple surveys across the winter, it is hard to determine whether change is predominantly from a~~
~~single event or not.~~ The response in summer is much smaller both in terms of deposition and erosion, with little morphological
change occurring ~~unsurprisingly.~~ What change does occur may be from reductions in bank support ~~from~~ after high flows
leaving banks exposed to collapse (Zhao et al., 2020).

1020 ~~Separating survey data by functional groups does not identify any dominant links between vegetation and morphological~~
~~change. Yet some of the effects were noticeable, including tree functional groups providing less winter stability than expected~~
~~based on previous research~~ (Gurnell, 2014; Hortobágyi et al., 2018). However, portions of the western end of the reach are
visibly stabilised by vegetation pinning (Figures 6 and 8), suggesting a mixed effect on morphological change. The lack of any
clear pattern could be due to a number of factors. Primarily, the relatively short nature of the study period at 2 years is not
necessarily long enough to provide certainty in any feedbacks occurring. In addition, errors in the reconstruction, separation,
and classification, could propagate through to suggest that the lack of clear pattern is due to the inability to classify functional
groups effectively at a reach scale. However, the vegetation reconstruction has proved to be effective both within this study
and others (e.g. Brede et al., 2019), producing model attributes in line with previously published values for the same species.
The accuracy of the classification was similar to other studies (e.g. Butterfield et al., 2020) and the majority of

misclassifications happened between similar groups. Finally, the lack of an obvious link could in part be due to the absence of data linking morphological change and vegetation with relevant flood inundation depths.

To assess the link between vegetation, morphological change and flood inundation, some simple further analysis was undertaken to explore the possibility of depth dependent drag being related to morphological change. Based upon the well-established relationship between submerged vegetation frontal area and drag (Nepf and Vivoni, 2000; Järvelä, 2004; Wilson et al., 2006; Gurnell, 2014) we estimated indicative excess drag for each functional group (except grass) at depths of 0.1, 0.5, 1, 2, and 4 metres for a hypothetical flood. In addition to the previously analysed herbaceous and tree point clouds, ten additional individual shrub point clouds were extracted to calculate average frontal area. To identify flow depths across the reach, a simple exploratory 2-D depth model in Delft3D (Deltares, 2021) was setup to extract hypothetical maximum flood depths across the study area using indicative flows taken from the gauge downstream of the study site for the Winter 2021 time period (Figure 1).

Within the modelled Delft3D water extent, the depth was used to extract the relevant frontal area interacting with the flow. Each of these depth dependent frontal areas were then used to determine the average excess drag component (F) of a single plant according to,

$$F = \frac{1}{2} C_D A_0 \rho U^2 \quad [1]$$

where C_D is the coefficient of drag, A_0 is the frontal area of the plant facing the flow, ρ is the fluid density, and U is the velocity of the fluid. It is difficult to identify any definitive links between the morphological change and vegetation presence, due to the limited time of study and the variations in vegetation extent and proximity to the channel. Yet, by aggregating the change across these various functional groups it was possible to see some of the effects of different groups, with areas such as grass consistently contributing to areas of erosion during the winter months, and tree groups undergoing just as much morphological change as herbaceous groups, despite their well known stabilising effects. approximated using Delft3D and a floodplain Manning's n of 0.035 to represent long grass. The excess drag for an individual plant was then transformed into an excess drag per metre squared, being multiplied by the plant density which was calculated using a local maximum filter to identify the top of individual plants, similar to the procedures used to delineate individual trees in dense canopies (Gurnell, 2014; Hortobágyi, Douss and Farah, 2022; Chen et al., 2018, 2020). Importantly, it is clear that looking through time to identify patterns is a challenge due to the inherent variability between seasons as can be seen by looking at the excess drag provided by each group between years. Changes in the spatial distribution and extent of different functional groups can alter the overall resistance across the floodplain, and in this case results in a drop in resistance from one season to the next. Moreover, being able to adjust

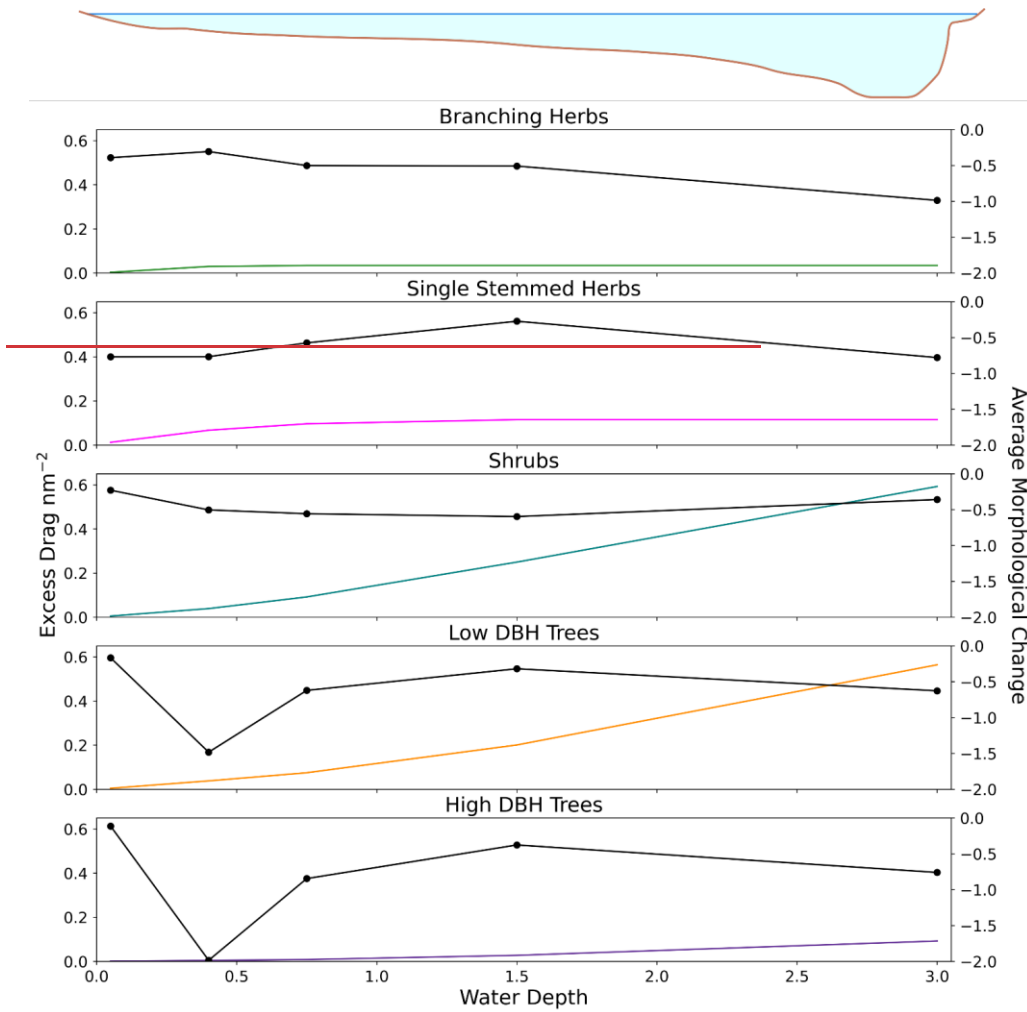
these for both summer and winter periods gives a greater insight in to the fluctuations in the influence of vegetation across a domain, and should continue to be accounted for when investigating the influence of vegetation on flow (REFS).

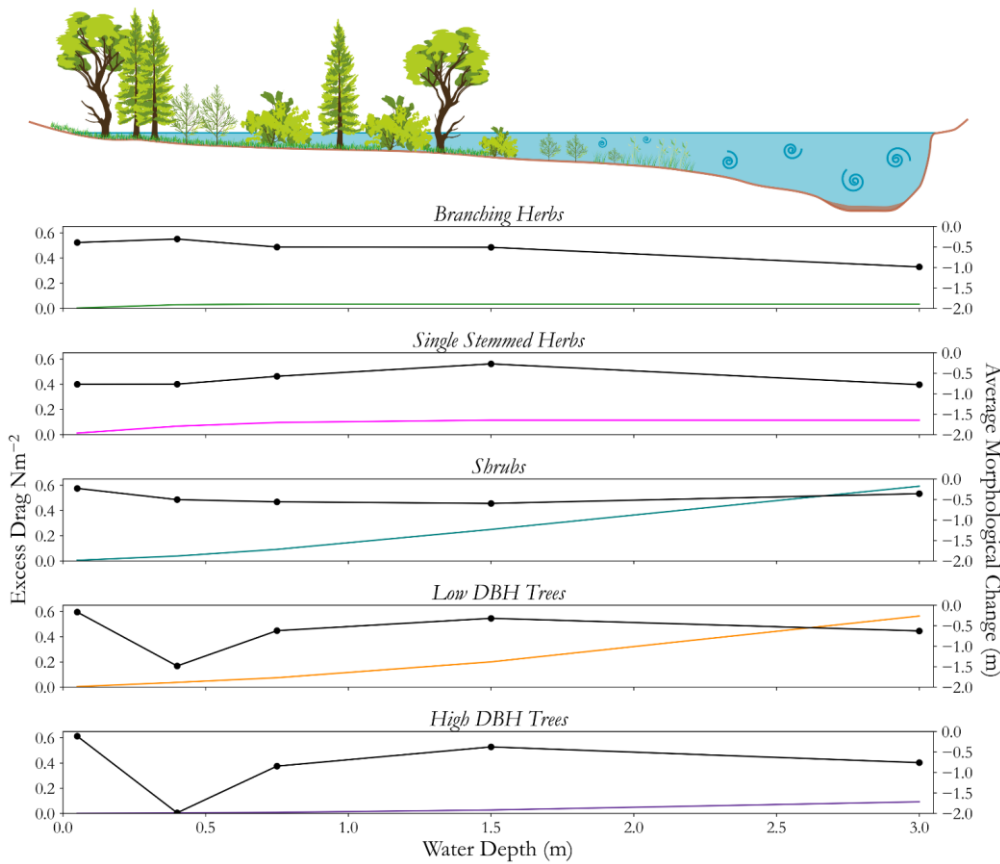
1060 The current analysis investigated a two strand approach, by comparing the functional groups to morphological change, and the excess drag across the domain created by each functional group. However, investigating the morphological change compared to depth dependent drag is challenging. This is also spatially and temporally varying with different flow routines and patterns. However, for the flood event used to predict flow depths, the morphological change experienced over that time period can be compared to each functional groups excess drag, and the impact this had on subsequent morphology.

1065 Figure X illustrates the changing excess drag provided by each functional group at different flow depths, and the equivalent morphological change experienced at these locations for the winter of 2021/22. However this approximation does not account for differences in drag caused by variations in the density and distribution of biomass. (James et al., 2008; Sand-Jensen, 2008). Drag coefficients were estimated based on morphology and values from the wider literature (see supplementary material). As a result, spatially varying excess drag was approximated across the domain for the winter of 2021 based on an indicative maximum flood extent. This can be used to compare the morphological change to spatially varying estimates of excess drag (Figure 11), demonstrating the excess drag and aggregated morphological change for each functional group, for each binned flow depth.

1075 All functional groups do see exhibit an increase in erosion with greater flow depths as would be expected, implying that the variation in erosion patterns seen across the range in flow depths may be in part due to the function of the vegetation. For both herbaceous guilds, as expected the influence of the plant form on flow increases due to the increases in shear stress with depth (e.g. Biron et al., 2004; Phillips, 2015). Yet for herbaceous groups, erosion rates are stable or decrease up until their maximum heights, and that for both of these groups the levels of erosion reduce up until below this maximum height, and past this levels of erosion increase. Clearly, at greater flow depths the shear stress on the bed will increase (REFS) and as such induce greater levels of erosion, but as this trend is not linear in nature with increasing depth, it suggests that herbaceous guilds are having an impact on flow and subsequent morphological change within the reach over this time period the maximum plant heights (see Figure 6) whereby erosion increases again, suggesting possible moderation due to the vegetation. The remaining three functional groups will all see consistently increasing levels of excess drag as their height is greater than the maximum interacted flow across flow depths. Shrubs frontal area increase quicker with flow depth as the branching network becomes more complex with a greater presence of foliage. The difference in drag experienced by the low and high-DBH guilds is predominantly the result of density differences again, as the plant heights exceed the maximum depth. Shrubs show the most consistent morphological stability, most likely due to their ability to reduce flow speeds, and the root structures of larger nature of the vegetation providing greater soil cohesion. Both sets of tree groups follow a similar pattern, appearing to accelerate erosion at

low flow depths, before being stabilised showing a stabilising effect at greater depth, some of which may be in part due to the poor ability to classify understory vegetation and as such miss, missing some of the variation/variability in these areas.





095 **Figure X11.** A comparison of how for each separate functional group, the approximated excess drag (coloured lines, no dots) and morphological response (black line, dotted) changes with hypothetical flow depth. The diagram cartoon at the top helps to illustrate how for different groups, different flow depths result result in different proportions of the plant influencing/interacting with flow.

This begins to raise interesting questions around the coupled nature of flow and vegetation, and at what point does one thresholds above which vegetation may begin to dominant/dominate in dictating the direction of geomorphic evolution. The exploratory analysis undertaken here begins to untangle/investigate this by using structural data across the domain to determine/estimate the vegetations influence of vegetation at hypothetical flow depths seen in the field during an observed flood event, whilst also using/comparing these to real changes in morphology. Although the drag calculations are averaged for the entire functional group, and the morphological signal being used is an average, this provides a new and promising avenue of

research which could relate ~~an~~ individual ~~plants~~ plant influence on various flood stages and the subsequent morphological ~~form~~ response of the channel.

6. Remote Sensing of Plant Functional Traits: What Next?

One of the key benefits of ~~using~~ remote sensing is the ability to quickly capture datasets over scales not possible with ground-based surveying. ~~It is clear from the analysis herein that although~~ Although the collection of ~~the data used~~ is fairly straightforward, the subsequent post-processing ~~time has to~~ must be ~~taken into account. Yet one~~ accounted for when ~~considering the routine application of a traits-based approach. Once~~ data has been processed, ~~and the seasonality of the data acquired through spectral and structural characteristics,~~ the success of the classification suggests that functional groups can be classified for other sites that contain similar vegetation in much the same way as ~~other previous traits-based~~ research has ~~used previous classes for similar environmental conditions before~~ done (e.g. Butterfield et al., 2020). ~~It also allows for functional groups to be mapped~~ Moreover, such methods may benefit areas in ~~regions that are which~~ ground-based surveying is more ~~remote and less accessible to more traditional surveys. This improves~~ challenging, improving the applicability and usability of ~~trait-based~~ methods when compared to ~~more~~ traditional taxonomic ~~vegetation discretisation~~ approaches. ~~However, further assessment comparing ground based with remotely sensed trait collection is still required.~~

Combining ~~vegetation~~ structural and spectral data provides the opportunity to upscale ~~to~~ datasets collected via other platforms, ~~with such as~~ high resolution satellite imagery and ALS datasets ~~offering the potential to improve the impact of such classification methods.~~ Currently, the main difficulty with traits-based analysis is ~~getting~~ collecting adequate data over large enough areas, ~~this~~. The methodology developed here provides a potential starting point from which a set of tools to classify different hydraulically relevant functional groups across larger areas can be ~~based~~ developed. This may overcome some of the scale issues in linking ~~guilds~~ vegetation functional groups to geomorphic change, whereby not enough data to link directions of change with different functional groups has ~~been collected. Currently most large-scale studies link evolution to vegetation presence, and small studies are too localised to be applicable across wider areas. This research which begins to explore the links between different functional groups and morphological evolution, demonstrates that by upscaling to combine enough hydraulic and morphological conditions may allow this to be possible~~ previously been collected.

~~Despite the variation in spatial variation between years and the variation in hydraulic influence between seasons being accounted for, an aspect of vegetation that is of great importance is the life cycle of vegetation. During this time, the functional role vegetation plays within the river system changes. Future work may also consider how vegetation is represented, and how temporally these representations change. For example, the role that large trees play when they are uprooted significantly changes, of vegetation changes from a establishment, maturity, and removal over the course of a plants life. Large trees for example, transition from stabilising feature for river banks during maturity, to one that increases channel roughness and~~

turbulence, dramatically altering in channel flow directions, and lead to subsequent morphological impacts when removed into the river system (Jeffries et al., 2003; Sear et al., 2010). Therefore, when classifying regions into functional groups, it may be necessary to consider that these are dynamic classes which vary through time. How we begin to monitor and detect these shifts in groups is an area of future research, especially in terms of woody debris which greatly contribute to the dynamics of fluvial systems;

One of the challenges of traits based approaches is the ability to collect widespread data as outlined previously. The classification inputs used predominantly focussed on structural and spectral characteristics of the vegetation, and as a result require advanced data collection techniques. However, it is widely shown that traits vary dependent on their underlying hydraulic and environmental conditions (e.g. Göthe et al., 2017; Corenblit et al., 2015). It is therefore not inconceivable that Likewise, the inclusion of layers such metrics may be used in future, such as to show as inundation frequency or extent, alongside flow velocity may improve classification approaches, with different traits being dependent on hydraulic and environmental conditions (Göthe et al., 2017; Corenblit et al., 2015). Moreover, both shrubs and grasses are key elements of UK and other temperate river systems, and remote sensing methods will struggle to capture their complexity due to the sensors limits of detection, currently relying on species identification from imagery or the field (Butterfield et al., 2020) to determine the likely composition of traits. This may take a more holistic approach and in cases where less structural data is present, allow for a more robust classification of guilds.

There alternative, As such, approaches will also be necessary when the limit of trait detection is reached from remote sensing. Variations in traits undetectable from TLS or UAV LS methods will limit the ability to detect features for certain types of functional groups, such as those too small to resolve or those with too complex structures, such as for grasses and branching shrubs. Both of these are prominent features of UK river corridors and so to improve their omission from current analysis is a limitation. The current integration into the methods can still map their extents but would require in field trait collection or the use of trait databases (e.g. TRY presented here (Kattge, G. Manners et al., 2020, 2013)) which are known to have their limitations. Yet species identification can be achieved with platforms cheaper than those used in this study, and supplemented with in field data assuming access to the site is safe. A key discussion point tends to revolve around how much data is required? Within this study, the repeat surveying was used to better group and map the extents of different vegetation, yet it is not always possible to collect such quantities of data. The analysis above would suggest that the seasonality of data collection plays a critical role, with tree species being better separated in the winter, due to the leaf off conditions providing better conditions for identifying overall structure, whilst summer surveys better capture the extent of different herbaceous groups. As a result, it is unlikely that a singular time frame is best for to be of benefit to wider eco-geomorphic research. Finally, in order to reduce the limitations of combining winter and following summer data, capturing such variety, and in order for traits based approaches to become common using remote sensing data frequently to enable 4D analysis of how vegetation properties change through time will enable further work to identify optimal timings for data collection needs to be investigations into eco-geomorphic

170 feedbacks beyond what has been undertaken in this study, particularly focussing on changes occurring during specific geomorphic events.

7. Conclusion

175 In this study, we have presented a novel method for collecting and extracting vegetation functional trait data that is relevant to eco-geomorphic research. Herein we used UAV-LS and UAV-MS datasets to advance our ability to collect high-resolution 4D datasets, improving the spatial and temporal resolution of riparian vegetation monitoring and geomorphic change detection. This has allowed us to gain an insight into how the influence of riparian vegetation changes through time and to better discretise the spatial variation of vegetation into functional groups which are scaleable. As such, we have been able to provide insight in to how traits-based frameworks for vegetation analysis can be linked to trends and patterns in morphological evolution at scales that were previously not attainable. We have also outlined the limits for current trait extraction from remote sensing techniques. UAV-LS can characterise larger vegetation structures and be used to upscale local TLS models, but even TLS is limited in its ability to characterise the spatial complexity of some vegetation traits at the resolution required to extract traits which can be linked with geomorphic change. This builds on current research which has analysed ecogeomorphic interactions on small river sections, or used species-based imagery classification to investigate geomorphic variations. The use of remote sensing allows data to be captured, analysed, related to broader dataset statistics, and upscaled to include larger reaches. 180 Simultaneously, the same data allows for the collection of topographic responses to flow events which can be linked to the variation in vegetation. This analysis uses seasonality to improve the classification of guilds via changes in structural and spectral properties, advancing current methods available to the ecogeomorphology community. The trait data can then be used to infer changes in excess drag across the reach, and also be linked to specific flow events to investigate how vegetation type and interaction with differing flows affects geomorphic response. Despite some noted limitations, this research represents an important step towards better discretisation of traits across greater scales and the furthers the possibility of implementing widespread traits-based research. 185

190 Future research is needed to investigate the limits of various remote sensing methods in relation to their ability to be used for traits extraction and thereby improve understanding of a system's ecogeomorphic evolution, with a focus on high-resolution land cover data, remote sensing imagery, and ALS. Likewise, a need to advance the relationship between vegetation, morphology, and flow interaction is required, accounting for the spatial variations in flow depths, and therefore what elements of individual plants are interacting with the flow. This is especially important when examining the variation within different functional groups and across different hydrological regimes. These methods offer a bridge across scales, within which to consider the ways in which riparian vegetation within the river corridor is mapped, evaluated, and modelled through time, with implications for establishing new insights into the functioning of eco-geomorphic systems across scales. 195 200

205

210 This study has presented a methodological workflow to extract vegetation traits within a river corridor from remotely sensed data, before creating functional groups that can be compared to geomorphic change. This presents an important advance in relation to current methods which use species identification from ground surveys or aerial imagery, instead scaling individual plant data to reach scale classifications. The use of leaf-on and leaf-off surveys enabled the separation of functional groups across the reach, highlighting the benefits of a seasonal approach when utilising remote sensing for vegetation mapping.
215 Despite not identifying discernible directions or magnitudes of geomorphic change between different functional groups, the methods used can still provide a template for future research into eco-geomorphic interactions. Exploratory analysis between depth related drag and morphological evolution highlighted the potential of using such approaches in the future, where vegetation function and the proximity and interaction with flow can be taken into account.

220 The potential of UAV-LS for river corridor research is considerable, capturing elements of topography and vegetation simultaneously in ways which are not possible from current SfM approaches alone. In addition, the combination of UAV-LS and SfM data enables greater confidence in the spatial representation of vegetation types and morphological change throughout the river corridor. This is especially pertinent given the seasonal approach employed in this study, where repeat surveying of the reach could be undertaken efficiently without the need for extensive ground surveying. However, this does not replace the
225 need for ground based methods, with species identification and TLS being used to supplement aerial datasets. These will continue to be required for vegetation groups that are either too small to be captured at the plant scale or too complex to capture their traits from UAV platforms. This is an area of research that requires further investigation, allowing for improved integration between remotely sensed and ground-based data. The methods presented herein offer a way in which to address the current gap between individual plant scale trait analysis and reach scale functional groups classification, allowing traits-
230 based approaches to be applied to other river reaches of similar scale or greater, enabling greater insight to be gained in relation to eco-geomorphic interactions within the river corridor and beyond.

Data Availability

The raw data ~~used~~ collected and analysed in this analysis is available at <https://zenodo.org/record/5529739#.YbDLBtDP1PY>

Author Contributions

1235 Study conceptualisation was done by C.T. and J.L. Data collection was undertaken by C.T. and J.L. Processing and data analysis was performed by C.T., with supervision from J.L. Original draft preparation by C.T. with reviewing and editing by C.T. and J.L. All authors have read and agreed to the published version of the manuscript.

Competing Interests

The authors declare that they have no conflict of interest.

1240 Acknowledgements

This research was funded by the Natural Environment Research Council (NERC), grant number 1937474 via PhD studentship support to CT as part of the Next Generation Unmanned System Science (NEXUSS) Centre for Doctoral Training, hosted at University of Southampton. [We thank the editors and two anonymous reviewers for thorough comments and suggestions which significantly improved the focus and narrative of the paper.](#)

1245 8. References

- Abeleira Martínez, O. J., Fremier, A. K., Günter, S., Ramos Bendaña, Z., Vierling, L., Galbraith, S. M., [Bosque-Pérez, N. A., and . . . Ordoñez, J. C.](#): Scaling up functional traits for ecosystem services with remote sensing: concepts and methods, *Ecol. Evol.*, 6, 4359-4371, <https://doi.org/10.1002/ece3.2201>, 2016.
- Abernethy, B. and Rutherford, I. D.: The distribution and strength of riparian tree roots in relation to riverbank reinforcement, *Hydrol. Process.*, 15, 63-79, <https://doi.org/10.1002/hyp.152>, 2001.
- Adam, E. and Mutanga, O.: Spectral discrimination of papyrus vegetation (*Cyperus papyrus* L.) in swamp wetlands using field spectrometry, *ISPRS Journal of Photogrammetry and Remote Sensing*, 64, 612-620, <https://doi.org/10.1016/j.isprsjprs.2009.04.004>, 2009.
- 1250 Adelabu, S. and Dube, T.: Employing ground and satellite-based QuickBird data and random forest to discriminate five tree species in a Southern African Woodland, *Geocarto International*, 30, 457-471, 10.1080/10106049.2014.885589, 2015.
- Aguiar, F. C., Segurado, P., Martins, M. J., Bejarano, M. D., Nilsson, C., Portela, M. M., and Merritt, D. M.: The abundance and distribution of guilds of riparian woody plants change in response to land use and flow regulation, *J. Appl. Ecol.*, 55, 2227-2240, 10.1111/1365-2664.13110, 2018.
- 1260 Aguirre-Gutiérrez, J., Rifai, S., Shenkin, A., Oliveras, I., Bentley, L. P., Svátek, M., . . . Malhi, Y.: Pantropical modelling of canopy functional traits using Sentinel-2 remote sensing data, *Remote Sens. Environ.*, 252, 112122, <https://doi.org/10.1016/j.rse.2020.112122>, 2021.
- Al-Ali, Z. M., Abdullah, M. M., Asadalla, N. B., and Gholoum, M.: A comparative study of remote sensing classification methods for monitoring and assessing desert vegetation using a UAV-based multispectral sensor, *Environ. Monit. Assess.*, 192, 389, 10.1007/s10661-020-08330-1, 2020.

- 1265 Alaibakhsh, M., Emelyanova, I., Barron, O., Sims, N., Khiadani, M., and Mohyeddin, A.: Delineation of riparian vegetation from Landsat multi-temporal imagery using PCA, *Hydrol. Process.*, 31, 800-810, <https://doi.org/10.1002/hyp.11054>, 2017.
- Anderson, K. E., Glenn, N. F., Spaete, L. P., Shinneman, D. J., Pilliod, D. S., Arkle, R. S., ~~McIlroy, S. K., and . . .~~ Derryberry, D. R.: Estimating vegetation biomass and cover across large plots in shrub and grass dominated drylands using terrestrial lidar and machine learning, *Ecol. Indic.*, 84, 793-802, <https://doi.org/10.1016/j.ecolind.2017.09.034>, 2018.
- 1270 Antonarakis, A. S., Richards, K. S., and Brasington, J.: Object-based land cover classification using airborne LiDAR, *Remote Sens. Environ.*, 112, 2988-2998, <https://doi.org/10.1016/j.rse.2008.02.004>, 2008.
- ~~Baatrup-Pedersen, A., Larsen, S. E., and Riis, T.: Long-term effects of stream management on plant communities in two Danish lowland streams, *Hydrobiologia*, 481, 33-45, 10.1023/a:1021296519187, 2002.~~
- ~~Baatrup-Pedersen, A., Göthe, E., Riis, T., and O'Hare, M. T.: Functional trait composition of aquatic plants can serve to disentangle multiple interacting stressors in lowland streams, *Science of The Total Environment*, 543, 230-238, <https://doi.org/10.1016/j.scitotenv.2015.11.027>, 2016.~~
- ~~Baatrup-Pedersen, A., Gothe, E., Larsen, S. E., O'Hare, M., Birk, S., Riis, T., and Friberg, N.: Plant trait characteristics vary with size and eutrophication in European lowland streams, *J. Appl. Ecol.*, 52, 1617-1628, 10.1111/1365-2664.12509, 2015.~~
- 1275 ~~Baatrup-Pedersen, A., Garssen, A., Gothe, E., Hoffmann, C. C., Oddershede, A., Riis, T., van Bodegom, P. M., Larsen, S. E., and Soons, M.: Structural and functional responses of plant communities to climate change mediated alterations in the hydrology of riparian areas in temperate Europe, *Ecol. Evol.*, 8, 4120-4135, 10.1002/ece3.3973, 2018.~~
- ~~Bankhead, N. L., Thomas, R. E., and Simon, A.: A combined field, laboratory and numerical study of the forces applied to, and the potential for removal of, bar-top vegetation in a braided river, *Earth Surf. Process. Landf.*, 42, 439-459, <https://doi.org/10.1002/esp.3997>, 2017.~~
- 1285 Bertoldi, W., Drake, N. A., and Gurnell, A. M.: Interactions between river flows and colonizing vegetation on a braided river: exploring spatial and temporal dynamics in riparian vegetation cover using satellite data, *Earth Surf. Process. Landf.*, 36, 1474-1486, <https://doi.org/10.1002/esp.2166>, 2011.
- Bertoldi, W., Welber, M., Gurnell, A. M., Mao, L., Comiti, F., and Tal, M.: Physical modelling of the combined effect of vegetation and wood on river morphology, *Geomorphology*, 246, 178-187, <https://doi.org/10.1016/j.geomorph.2015.05.038>, 2015.
- 1290 ~~Biron, P. M., Robson, C., Lapointe, M. F., and Gaskin, S. J.: Comparing different methods of bed shear stress estimates in simple and complex flow fields, *Earth Surf. Process. Landf.*, 29, 1403-1415, <https://doi.org/10.1002/esp.1111>, 2004.~~
- ~~Blondel, J.: Guilds or functional groups: does it matter?, *Oikos*, 100, 223-231, <https://doi.org/10.1034/j.1600-0706.2003.12152.x>, 2003.~~
- 1295 ~~Blöschl, G., Ardoin-Bardin, S., Bonell, M., Dorninger, M., Goodrich, D., Gutknecht, D., . . . Szolgay, J.: At what scales do climate variability and land cover change impact on flooding and low flows?, *Hydrol. Process.*, 21, 1241-1247, <https://doi.org/10.1002/hyp.6669>, 2007.~~
- ~~Boothroyd, R. J., Hardy, R. J., Warburton, J., and Marjoribanks, T. I.: The importance of accurately representing submerged vegetation morphology in the numerical prediction of complex river flow, *Earth Surf. Process. Landf.*, 41, 567-576, <https://doi.org/10.1002/esp.3871>, 2016.~~
- 1300 ~~Brasington, J., Vericat, D., and Rychkov, I.: Modeling river bed morphology, roughness, and surface sedimentology using high resolution terrestrial laser scanning, *Water Resources Research*, 48, 18, 10.1029/2012wr012223, 2012.~~

- 1305 Brede, B., Calders, K., Lau, A., Raunonen, P., Bartholomeus, H. M., Herold, M., and Kooistra, L.: Non-destructive tree volume estimation through quantitative structure modelling: Comparing UAV laser scanning with terrestrial LIDAR, *Remote Sens. Environ.*, 233, 111355, <https://doi.org/10.1016/j.rse.2019.111355>, 2019.
- Brodu, N. and Lague, D.: 3D terrestrial lidar data classification of complex natural scenes using a multi-scale dimensionality criterion: Applications in geomorphology, *ISPRS Journal of Photogrammetry and Remote Sensing*, 68, 121-134, <https://doi.org/10.1016/j.isprsjprs.2012.01.006>, 2012.
- 1310 Burgess, P., Graves, A., deDe Jalón, S. G., Palma, J., Dupraz, C., and van Van Noordwijk, M.: Modelling agroforestry systems, in: *Agroforestry for sustainable agriculture*, Burleigh Dodds Science Publishing, 209-238, 2019.
- Burt, A., Disney, M., and Calders, K.: Extracting individual trees from lidar point clouds using treeseg, *Methods in Ecology and Evolution*, 10, 438-445, 2019.
- Butterfield, B. J., Grams, P. E., Durning, L. E., Hazel, J., Palmquist, E. C., Ralston, B. E., and Sankey, J. B.: Associations between riparian plant morphological guilds and fluvial sediment dynamics along the regulated Colorado River in Grand Canyon, *River Research and Applications*, 36, 410-421, <https://doi.org/10.1002/rra.3589>, 2020.
- 1315 Bywater-Reyes, S., Wilcox, A., and Diehl, R.: Multiscale influence of woody riparian vegetation on fluvial topography quantified with ground-based and airborne lidar, *J. Geophys. Res.-Earth Surf.*, 122, 1218-1235, 10.1002/2016jfr004058, 2017.
- ~~Caponi, F., Vetsch, D. F., and Siviglia, A.: A model study of the combined effect of above and below ground plant traits on the geomorphodynamics of gravel bars, *Scientific Reports*, 10, 17062, 10.1038/s41598-020-74106-9, 2020.~~
- 1320 ~~Calders, K., Newnham, G., Burt, A., Murphy, S., Raunonen, P., Herold, M., . . . Kaasalainen, M.: Nondestructive estimates of above-ground biomass using terrestrial laser scanning, *Methods in Ecology and Evolution*, 6, 198-208, <https://doi.org/10.1111/2041-210X.12301>, 2015.~~
- Chen, J. C.-W. and Paelinckx, D.: Evaluation of Random Forest and Adaboost tree-based ensemble classification and spectral band selection for ecotope mapping using airborne hyperspectral imagery, *Remote Sens. Environ.*, 112, 2999-3011, <https://doi.org/10.1016/j.rse.2008.02.011>, 2008.
- 1325 Chen, W., Xiang, H., and Moriya, K.: Individual Tree Position Extraction and Structural Parameter Retrieval Based on Airborne LiDAR Data: Performance Evaluation and Comparison of Four Algorithms, *Remote Sensing*, 12, 571, 2020.
- Colbert, K. C., Larsen, D. R., and Lootens, J. R.: Height-Diameter Equations for Thirteen Midwestern Bottomland Hardwood Species, *Northern Journal of Applied Forestry*, 19, 171-176, 10.1093/njaf/19.4.171, 2002.
- 1330 Corenblit, D., Baas, A., Balke, T., Bouma, T., Fromard, F., Garófano-Gómez, V., . . . Walcker, R.: Engineer pioneer plants respond to and affect geomorphic constraints similarly along water-terrestrial interfaces world-wide, *Global Ecology and Biogeography*, 24, 1363-1376, 10.1111/geb.12373, 2015.
- Coulthard, T. J.: Effects of vegetation on braided stream pattern and dynamics, *Water Resources Research*, 41, <https://doi.org/10.1029/2004WR003201>, 2005.
- 1335 Crosato, A. and Saleh, M. S.: Numerical study on the effects of floodplain vegetation on river planform style, *Earth Surf. Process. Landf.*, 36, 711-720, <https://doi.org/10.1002/esp.2088>, 2011.
- Dalla Corte, A. P., deDe Vasconcellos, B. N., Rex, F. E., Sanquetta, C. R., Mohan, M., Silva, C. A., . . . Broadbent, E. N.: Applying High-Resolution UAV-LiDAR and Quantitative Structure Modelling for Estimating Tree Attributes in a Crop-Livestock-Forest System, *Land*, 11, 507, 2022.

- 1340 [Dash, J. P., Watt, M. S., Paul, T. S. H., Morgenroth, J., and Pearse, G. D.: Early Detection of Invasive Exotic Trees Using UAV and Manned Aircraft Multispectral and LiDAR Data, *Remote Sensing*, 11, 1812, 2019.](#)
- De Baets, S., Poesen, J., Knapen, A., Barberá, G. G., and Navarro, J.: Root characteristics of representative Mediterranean plant species and their erosion-reducing potential during concentrated runoff, *Plant and Soil*, 294, 169-183, 2007.
- 1345 De Bello, F., Lepš, J., and Sebastià, M. T.: Variations in species and functional plant diversity along climatic and grazing gradients, *Ecography*, 29, 801-810, 2006.
- De Doncker, L., Troch, P., Verhoeven, R., Bal, K., Desmet, N., and Meire, P.: Relation between resistance characteristics due to aquatic weed growth and the hydraulic capacity of the river Aa, *River Research and Applications*, 25, 1287-1303, <https://doi.org/10.1002/rra.1240>, 2009.
- [Deltares: Delft3D-FLOW User Manual, 2021.](#)
- 1350 [Dersch, S., Schöttl, A., Krzystek, P., and Heurich, M.: Towards complete tree crown delineation by instance segmentation with Mask R-CNN and DETR using UAV-based multispectral imagery and lidar data, *ISPRS Open Journal of Photogrammetry and Remote Sensing*, 8, 100037, <https://doi.org/10.1016/j.ojphoto.2023.100037>, 2023.](#)
- Diehl, R. M., Merritt, D. M., Wilcox, A. C., and Scott, M. L.: Applying Functional Traits to Ecogeomorphic Processes in Riparian Ecosystems, *Bioscience*, 67, 729-743, 10.1093/biosci/bix080, 2017a.
- 1355 Diehl, R. M., Wilcox, A. C., Merritt, D. M., Perkins, D. W., and Scott, J. A.: Development of an eco-geomorphic modeling framework to evaluate riparian ecosystem response to flow-regime changes, *Ecological Engineering*, 123, 112-126, <https://doi.org/10.1016/j.ecoleng.2018.08.024>, 2018.
- Diehl, R. M., Wilcox, A. C., Stella, J. C., Kui, L., Sklar, L. S., and Lightbody, A.: Fluvial sediment supply and pioneer woody seedlings as a control on bar-surface topography, *Earth Surf. Process. Landf.*, 42, 724-734, <https://doi.org/10.1002/esp.4017>, 2017b.
- 1360 [Donoghue, D. N. M., Watt, P. J., Cox, N. J., and Wilson, J.: Remote sensing of species mixtures in conifer plantations using LiDAR height and intensity data, *Remote Sens. Environ.*, 110, 509-522, <https://doi.org/10.1016/j.rse.2007.02.032>, 2007.](#)
- Douss, R. and Farah, I. R.: Extraction of individual trees based on Canopy Height Model to monitor the state of the forest, *Trees, Forests and People*, 8, 100257, <https://doi.org/10.1016/j.tfp.2022.100257>, 2022.
- 1365 Duro, D. C., Franklin, S. E., and Dube, M. G.: A comparison of pixel-based and object-based image analysis with selected machine learning algorithms for the classification of agricultural landscapes using SPOT-5 HRG imagery, *Remote Sens. Environ.*, 118, 259-272, 10.1016/j.rse.2011.11.020, 2012.
- Engindeniz, S. and Olgun, A.: Determination of land and tree values of hybrid poplar plantations: A case study for Turkey, *Southern African Forestry Journal*, 197, 31-38, 10.1080/20702620.2003.10431719, 2003.
- 1370 ESRI: Imagery [Basemap], Maxar Imagery (28/09/2014), 2021.
- Fang, R. and Strimbu, B. M.: Comparison of Mature Douglas-Firs' Crown Structures Developed with Two Quantitative Structural Models Using TLS Point Clouds for Neighboring Trees in a Natural Regime Stand, *Remote Sensing*, 11, 1661, 2019.
- Felzenszwalb, P. F. and Huttenlocher, D. P.: Efficient Graph-Based Image Segmentation, *International Journal of Computer Vision*, 59, 167-181, 10.1023/B:VISI.0000022288.19776.77, 2004.

- 375 [Follett, E. and Nepf, H.: Sediment patterns near a model patch of reedy emergent vegetation, *Geomorphology*, 179, 141–151, 10.1016/j.geomorph.2012.08.006, 2012.](#)
- Fox, G. A., Wilson, G. V., Simon, A., Langendoen, E. J., Akay, O., and Fuchs, J. W.: Measuring streambank erosion due to ground water seepage: correlation to bank pore water pressure, precipitation and stream stage, *Earth Surf. Process. Landf.*, 32, 1558-1573, 2007.
- 380 [Francalanci, S., Paris, E., and Solari, L.: On the vulnerability of woody riparian vegetation during flood events, *Environmental Fluid Mechanics*, 20, 635–661, 10.1007/s10652-019-09726-5, 2020.](#)
- Garnier, E., Lavorel, S., Ansquer, P., Castro, H., Cruz, P., Dolezal, J., . . . Zarovali, M. P.: Assessing the Effects of Land-use Change on Plant Traits, Communities and Ecosystem Functioning in Grasslands: A Standardized Methodology and Lessons from an Application to 11 European Sites, *Annals of Botany*, 99, 967-985, 10.1093/aob/mcl215, 2006.
- 1385 Gilvear, D., Tyler, A., and Davids, C.: Detection of estuarine and tidal river hydromorphology using hyper-spectral and LiDAR data: Forth estuary, Scotland, *Estuar. Coast. Shelf Sci.*, 61, 379-392, 10.1016/j.ecss.2004.06.007, 2004.
- Göthe, E., Baattrup-Pedersen, A., Wiberg-Larsen, P., Graeber, D., Kristensen, E. A., and Friberg, N.: Environmental and spatial controls of taxonomic versus trait composition of stream biota, *Freshwater Biology*, 62, 397-413, 10.1111/fwb.12875, 2017.
- 390 [Guo, X., Wang, M., Jia, M., and Wang, W.: Estimating mangrove leaf area index based on red-edge vegetation indices: A comparison among UAV, WorldView-2 and Sentinel-2 imagery, *International Journal of Applied Earth Observation and Geoinformation*, 103, 102493, <https://doi.org/10.1016/j.jag.2021.102493>, 2021.](#)
- Gurnell, A.: Plants as river system engineers, *Earth Surf. Process. Landf.*, 39, 4-25, 2014.
- Hackenberg, J., Spiecker, H., Calders, K., Disney, M., and Raunonen, P.: SimpleTree —An Efficient Open Source Tool to Build Tree Models from TLS Clouds, *Forests*, 6, 4245-4294, 2015.
- 1395 Harvey, J. and Gooseff, M.: River corridor science: Hydrologic exchange and ecological consequences from bedforms to basins, *Water Resources Research*, 51, 6893-6922, doi:10.1002/2015WR017617, 2015.
- 400 [Hillman, S., Wallace, L., Reinke, K., and Jones, S.: A comparison between TLS and UAS LiDAR to represent eucalypt crown fuel characteristics, *ISPRS Journal of Photogrammetry and Remote Sensing*, 181, 295-307, <https://doi.org/10.1016/j.isprsjprs.2021.09.008>, 2021.](#)
- Hortobágyi, B., Corenblit, D., Steiger, J., and Peiry, J.-L.: Niche construction within riparian corridors. Part I: Exploring biogeomorphic feedback windows of three pioneer riparian species (Allier River, France), *Geomorphology*, 305, 94-111, <https://doi.org/10.1016/j.geomorph.2017.08.048>, 2018.
- 1405 Hortobágyi, B., Corenblit, D., Ding, Z., Lambs, L., and Steiger, J.: Above-and belowground responses of *Populus nigra* L. to mechanical stress observed on the Allier River, France, *Géomorphologie: relief, processus, environnement*, 23, 219-231, 2017.
- Houborg, R., Fisher, J. B., and Skidmore, A. K.: Advances in remote sensing of vegetation function and traits, *International Journal of Applied Earth Observation and Geoinformation*, 43, 1-6, <https://doi.org/10.1016/j.jag.2015.06.001>, 2015.
- 410 [Huang, H.-Q. and Nanson, G. C.: The influence of bank strength on channel geometry: an integrated analysis of some observations, *Earth Surf. Process. Landf.*, 23, 865–876, \[61\]\(https://doi.org/10.1002/\(SICI\)1096-9837\(199810\)23:10<865::AID-ESP903>3.0.CO;2-3, 1998.</p></div><div data-bbox=\)](#)

Hughes, A. O.: Riparian management and stream bank erosion in New Zealand, *New Zealand Journal of Marine and Freshwater Research*, 50, 277-290, [10.1080/00288330.2015.1116449](https://doi.org/10.1080/00288330.2015.1116449), 2016.

Hupp, C. R. and Osterkamp, W.: Riparian vegetation and fluvial geomorphic processes, *Geomorphology*, 14, 277-295, 1996.

1415 [Hyypä, E., Yu, X., Kaartinen, H., Hakala, T., Kukko, A., Vastaranta, M., and Hyypä, J.: Comparison of Backpack, Handheld, Under-Canopy UAV, and Above-Canopy UAV Laser Scanning for Field Reference Data Collection in Boreal Forests, *Remote Sensing*, 12, 3327, 2020.](https://doi.org/10.1016/j.rse.2020.107327)

Jalonen, J., Järvelä, J., and Aberle, J.: Leaf area index as vegetation density measure for hydraulic analyses, *Journal of Hydraulic Engineering*, 139, 461-469, 2012.

1420 [Jalonen, J., Jarvela, J., Virtanen, J. P., Vaaja, M., Kurkela, M., and Hyypä, H.: Determining Characteristic Vegetation Areas by Terrestrial Laser Scanning for Floodplain Flow Modeling, *Water*, 7, 420-437, \[10.3390/w7020420\]\(https://doi.org/10.3390/w7020420\), 2015.](https://doi.org/10.3390/w7020420)

James, C. S., Goldbeck, U. K., Patini, A., and Jordanova, A. A.: Influence of foliage on flow resistance of emergent vegetation, *Journal of Hydraulic Research*, 46, 536-542, [10.3826/jhr.2008.3177](https://doi.org/10.3826/jhr.2008.3177), 2008.

Järvelä, J.: [Determination of flow resistance of vegetated channel banks and floodplains, *River Flow 2002*, 311-318, 2002a.](https://doi.org/10.1016/j.rse.2002.03.002)

1425 [Järvelä, J.: Flow resistance of flexible and stiff vegetation: a flume study with natural plants, *Journal of Hydrology*, 269, 44-54, \[https://doi.org/10.1016/S0022-1694\\(02\\)00193-2\]\(https://doi.org/10.1016/S0022-1694\(02\)00193-2\), \[2002b2002a\]\(https://doi.org/10.1016/S0022-1694\(02\)00193-2\).](https://doi.org/10.1016/S0022-1694(02)00193-2)

[Järvelä, J.: Determination of flow resistance of vegetated channel banks and floodplains, *River Flow 2002*, 311-318, 2002b.](https://doi.org/10.1016/j.rse.2002.03.002)

Järvelä, J.: Determination of flow resistance caused by non-submerged woody vegetation, *Int. J. River Basin Manag.*, 2, 61-70, [10.1080/15715124.2004.9635222](https://doi.org/10.1080/15715124.2004.9635222), 2004.

1430 Jeffries, R., Darby, S. E., and Sear, D. A.: The influence of vegetation and organic debris on flood-plain sediment dynamics: case study of a low-order stream in the New Forest, England, *Geomorphology*, 51, 61-80, [https://doi.org/10.1016/S0169-555X\(02\)00325-2](https://doi.org/10.1016/S0169-555X(02)00325-2), 2003.

[Julian, J. P. and Torres, R.: Hydraulic erosion of cohesive riverbanks, *Geomorphology*, 76, 193-206, <https://doi.org/10.1016/j.geomorph.2005.11.003>, 2006.](https://doi.org/10.1016/j.geomorph.2005.11.003)

1435 Jurekova, Z., Baranec, T., Paganová, V., Kotrla, M., and Elias, P.: Comparison of the ecological characteristic the willow-poplar floodplain forest fragments on the stands with different height of groundwater level, *ECOLOGY-BRATISLAVA-*, 27, 31, 2008.

Kang, R. S.: GEOMORPHIC EFFECTS OF MOSSES IN A LOW-ORDER STREAM IN FAIRFAX COUNTY, VIRGINIA, *Phys. Geogr.*, 33, 360-382, [10.2747/0272-3646.33.4.360](https://doi.org/10.2747/0272-3646.33.4.360), 2012.

1440 [Kankare, V., Holopainen, M., Vastaranta, M., Puttonen, E., Yu, X., Hyypä, J., . . . Alho, P.: Individual tree biomass estimation using terrestrial laser scanning, *ISPRS Journal of Photogrammetry and Remote Sensing*, 75, 64-75, <https://doi.org/10.1016/j.isprsjprs.2012.10.003>, 2013.](https://doi.org/10.1016/j.isprsjprs.2012.10.003)

Kattge, J., Diaz, S., Lavorel, S., Prentice, I. C., Leadley, P., Bönisch, G., . . . Wright, I. J.: TRY—a global database of plant traits, *Global change biology*, 17, 2905-2935, 2011.

1445 Kattge, J. and Bönisch, G. and Díaz, S. and Lavorel, S. and Prentice, I. C. and Leadley, P., . . . Wirth, C.: TRY plant trait database – enhanced coverage and open access, *Global Change Biology*, 26, 119-188, <https://doi.org/10.1111/gcb.14904>, 2020.

Formatted: English (United Kingdom)

- Kim, S. J. and Stoesser, T.: Closure modeling and direct simulation of vegetation drag in flow through emergent vegetation, *Water Resources Research*, 47, <https://doi.org/10.1029/2011WR010561>, 2011.
- 1450 Krisanski, S., Taskhiri, M. S., Gonzalez Aracil, S., Herries, D., Muneri, A., Gurung, M. B., ~~Montgomery, J., and . . .~~ Turner, P.: Forest Structural Complexity Tool—An Open Source, Fully-Automated Tool for Measuring Forest Point Clouds, *Remote Sensing*, 13, 4677, 2021.
- Kyle, G. and Leishman, M. R.: Plant functional trait variation in relation to riparian geomorphology: The importance of disturbance, *Austral Ecology*, 34, 793-804, 10.1111/j.1442-9993.2009.01988.x, 2009.
- 1455 Lague, D.: Chapter 8 - Terrestrial laser scanner applied to fluvial geomorphology, in: *Developments in Earth Surface Processes*, edited by: Tarolli, P., and Mudd, S. M., Elsevier, Amsterdam, The Netherlands, 231-254, <https://doi.org/10.1016/B978-0-444-64177-9.00008-4>, 2020.
- Lague, D., Brodu, N., and Leroux, J.: Accurate 3D comparison of complex topography with terrestrial laser scanner: Application to the Rangitikei canyon (NZ), *ISPRS journal of photogrammetry and remote sensing*, 82, 10-26, 2013.
- Lane, S. N.: Natural flood management, *Wiley Interdiscip. Rev.-Water*, 4, 14, 10.1002/wat2.1211, 2017.
- 1460 [Letard, M., Lague, D., Le Guennec, A., Lefèvre, S., Feldmann, B., Leroy, P., . . . Corpetti, T.: 3DMASC: Accessible, explainable 3D point clouds classification. Application to Bi-Spectral Topo-Bathymetric lidar data. 2023.](#)
- [Leyland, J., Hackney, C. R., Darby, S. E., Parsons, D. R., Best, J. L., Nicholas, A. P., . . . Lague, D.: Extreme flood-driven fluvial bank erosion and sediment loads: direct process measurements using integrated Mobile Laser Scanning \(MLS\) and hydro-acoustic techniques. *Earth Surf. Process. Landf.*, 42, 334-346, 10.1002/esp.4078, 2017.](#)
- 1465 [Lian, X., Zhang, H., Xiao, W., Lei, Y., Ge, L., Qin, K., . . . Chang, J.: Biomass Calculations of Individual Trees Based on Unmanned Aerial Vehicle Multispectral Imagery and Laser Scanning Combined with Terrestrial Laser Scanning in Complex Stands. *Remote Sensing*, 14, 4715, 2022.](#)
- [Liang, X., Hyyppä, J., Kukko, A., Kaartinen, H., Jaakkola, A., and Yu, X.: The Use of a Mobile Laser Scanning System for Mapping Large Forest Plots, *IEEE Geosci. Remote Sens. Lett.*, 11, 1504-1508, 10.1109/LGRS.2013.2297418, 2014.](#)
- 1470 Lightbody, A. F. and Nepf, H. M.: Prediction of near-field shear dispersion in an emergent canopy with heterogeneous morphology, *Environmental Fluid Mechanics*, 6, 477-488, 10.1007/s10652-006-9002-7, 2006.
- [Lukaes, B. A., E-Vojtko, A., Eros, T., Molnar, V. A., Szabo, S., and Gotzenberger, L.: Carbon forms, nutrients and water velocity filter hydrophyte and riverbank species differently: A trait-based study, *Journal of Vegetation Science*, 30, 471-484, 10.1111/jvs.12738, 2019.](#)
- 1475 Manners, R., Schmidt, J., and Wheaton, J. M.: Multiscalar model for the determination of spatially explicit riparian vegetation roughness, *J. Geophys. Res.-Earth Surf.*, 118, 65-83, 10.1029/2011jf002188, 2013.
- Manners, R. B., Wilcox, A. C., Kui, L., Lightbody, A. F., Stella, J. C., and Sklar, L. S.: When do plants modify fluvial processes? Plant-hydraulic interactions under variable flow and sediment supply rates, *Journal of Geophysical Research: Earth Surface*, 120, 325-345, <https://doi.org/10.1002/2014JF003265>, 2015.
- 1480 [McCoyMccoy-Sulentic, M. E., Kolb, T. E., Merritt, D. M., Palmquist, E., Ralston, B. E., Sarr, D. A., and Shafroth, P. B.: Changes in Community-Level Riparian Plant Traits over Inundation Gradients, Colorado River, Grand Canyon, *Wetlands*, 37, 635-646, 10.1007/s13157-017-0895-3, 2017.](#)

- McGill, B. J., Enquist, B. J., Weiher, E., and Westoby, M.: Rebuilding community ecology from functional traits, *Trends in ecology & evolution*, 21, 178-185, 2006.
- 1485 Michalowska, M. and Rapiński, J.: A Review of Tree Species Classification Based on Airborne LiDAR Data and Applied Classifiers, *Remote Sensing*, 13, 353, 2021.
- Millar, R. G. and Quick, M. C.: Stable Width and Depth of Gravel-Bed Rivers with Cohesive Banks, *Journal of Hydraulic Engineering*, 124, 1005-1013, doi:10.1061/(ASCE)0733-9429(1998)124:10(1005), 1998.
- 1490 Myint, S. W., Gober, P., Brazel, A., Grossman-Clarke, S., and Weng, Q.: Per-pixel vs. object-based classification of urban land cover extraction using high spatial resolution imagery, *Remote Sens. Environ.*, 115, 1145-1161, <https://doi.org/10.1016/j.rse.2010.12.017>, 2011.
- Naiman, R. J., Decamps, H., and Pollock, M.: THE ROLE OF RIPARIAN CORRIDORS IN MAINTAINING REGIONAL BIODIVERSITY, *Ecological Applications*, 3, 209-212, 10.2307/1941822, 1993.
- Naiman, R. J., Bechtold, J. S., Drake, D. C., Latterell, J. J., O'keefe, T. C., and Balian, E. V.: Origins, patterns, and importance of heterogeneity in riparian systems, in: *Ecosystem function in heterogeneous landscapes*, Springer, 279-309, 2005.
- 1495 Nallaperuma, B. and Asaeda, T.: The long-term legacy of riparian vegetation in a hydrogeomorphologically remodelled fluvial setting, *River Research and Applications*, 36, 1690-1700, <https://doi.org/10.1002/rra.3665>, 2020.
- Nepf, H. M. and Vivoni, E. R.: Flow structure in depth-limited, vegetated flow, *Journal of Geophysical Research: Oceans*, 105, 28547-28557, <https://doi.org/10.1029/2000JC900145>, 2000.
- 1500 O'Hare, J., O'Hare, M., Gurnell, A., Dunbar, M., Scarlett, P., and Laize, C.: Physical constraints on the distribution of macrophytes linked with flow and sediment dynamics in British rivers, *River Research and Applications*, 27, 671-683, 2011.
- O'Hare, M., Mountford, J., Maroto, J., and Gunn, I.: Plant traits relevant to fluvial geomorphology and hydrological interactions, *River Research and Applications*, 32, 179-189, 2016.
- O'Briain, R., Shephard, S., and Coghlan, B.: Pioneer macrophyte species engineer fine-scale physical heterogeneity in a shallow lowland river, *Ecological Engineering*, 102, 451-458, <https://doi.org/10.1016/j.ecoleng.2017.02.047>, 2017.
- 1505 Olsoy, P. J., Glenn, N. F., Clark, P. E., and Derryberry, D. R.: Aboveground total and green biomass of dryland shrub derived from terrestrial laser scanning, *ISPRS Journal of Photogrammetry and Remote Sensing*, 88, 166-173, <https://doi.org/10.1016/j.isprsjprs.2013.12.006>, 2014.
- Oorscot, M. v., Kleinhans, M., Geerling, G., and Middelkoop, H.: Distinct patterns of interaction between vegetation and morphodynamics, *Earth Surf. Process. Landf.*, 41, 791-808, <https://doi.org/10.1002/esp.3864>, 2016.
- 1510 Palmer, M. A., Lettenmaier, D. P., Poff, N. L., Postel, S. L., Richter, B., and Warner, R.: Climate change and river ecosystems: protection and adaptation options, *Environmental management*, 44, 1053-1068, 2009.
- Palmquist, E. C., Sterner, S. A., and Ralston, B. E.: A comparison of riparian vegetation sampling methods along a large, regulated river, *River Research and Applications*, 35, 759-767, 10.1002/rra.3440, 2019.
- 1515 Quétier, F., Lavorel, S., Thuiller, W., and Davies, I.: Plant trait based modeling assessment of ecosystem service sensitivity to land use change, *Ecological Applications*, 17, 2377-2386, 2007.
- Phillips, J. D.: Hydrologic and geomorphic flow thresholds in the Lower Brazos River, Texas, USA, *Hydrological Sciences Journal*, 60, 1631-1648, 10.1080/02626667.2014.943670, 2015.

- 1520 Raumonon, P., Kaasalainen, M., Åkerblom, M., Kaasalainen, S., Kaartinen, H., Vastaranta, M., ~~Holopainen, M., Disney, M., and . . .~~ Lewis, P.: Fast Automatic Precision Tree Models from Terrestrial Laser Scanner Data, *Remote Sensing*, 5, 491-520, 2013.
- Rivaes, R. P., Rodriguez-Gonzalez, P. M., Ferreira, M. T., Pinheiro, A. N., Politti, E., Egger, G., ~~Garcia-Arias, A., and . . .~~ Frances, F.: Modeling the Evolution of Riparian Woodlands Facing Climate Change in Three European Rivers with Contrasting Flow Regimes, *Plos One*, 9, 14, 10.1371/journal.pone.0110200, 2014.
- 1525 Roussel, J.-R., Auty, D., Coops, N. C., Tompalski, P., Goodbody, T. R. H., Meador, A. S., ~~Bourdon, J.-F., de Boissieu, F., and . . .~~ Achim, A.: lidR: An R package for analysis of Airborne Laser Scanning (ALS) data, *Remote Sens. Environ.*, 251, 112061, <https://doi.org/10.1016/j.rse.2020.112061>, 2020.
- Sand-Jensen, K.: Drag and reconfiguration of freshwater macrophytes, *Freshwater Biology*, 48, 271-283, <https://doi.org/10.1046/j.1365-2427.2003.00998.x>, 2003.
- 1530 Sand-Jensen, K.: Drag forces on common plant species in temperate streams: consequences of morphology, velocity and biomass, *Hydrobiologia*, 610, 307-319, 2008.
- Sand-Jensen, K. and Pedersen, O.: Velocity gradients and turbulence around macrophyte stands in streams, *Freshwater Biology*, 42, 315-328, 1999.
- Savage, V. M., Webb, C. T., and Norberg, J.: A general multi-trait-based framework for studying the effects of biodiversity on ecosystem functioning, *Journal of theoretical biology*, 247, 213-229, 2007.
- 1535 ~~Schuster, C., Förster, M., and Kleinschmit, B.: Testing the red edge channel for improving land-use classifications based on high-resolution multi-spectral satellite data, *Int. J. Remote Sens.*, 33, 5583-5599, 10.1080/01431161.2012.666812, 2012.~~
- Sear, D. A., Millington, C. E., Kitts, D. R., and Jeffries, R.: Logjam controls on channel:floodplain interactions in wooded catchments and their role in the formation of multi-channel patterns, *Geomorphology*, 116, 305-319, <https://doi.org/10.1016/j.geomorph.2009.11.022>, 2010.
- 1540 Sharpe, R. and James, C.: Deposition of sediment from suspension in emergent vegetation, *Water Sa*, 32, 211-218, 2006.
- Simon, A., Curini, A., Darby, S. E., and Langendoen, E. J.: Bank and near-bank processes in an incised channel, *Geomorphology*, 35, 193-217, 2000.
- Southall, E., Dale, M. P., and Kent, M.: Floristic variation and willow carr development within a southwest England wetland, *Appl. Veg. Sci.*, 6, 63-72, <https://doi.org/10.1111/j.1654-109X.2003.tb00565.x>, 2003.
- 1545 Souza, J. and Hooke, J.: Influence of seasonal vegetation dynamics on hydrological connectivity in tropical drylands, *Hydrol. Process.*, 35, e14427, <https://doi.org/10.1002/hyp.14427>, 2021.
- ~~Stackhouse, L. A., Coops, N. C., White, J. C., Tompalski, P., Hamilton, J., and Davis, D. J.: Characterizing riparian vegetation and classifying riparian extent using airborne laser scanning data, *Ecol. Indic.*, 152, 110366, <https://doi.org/10.1016/j.ecolind.2023.110366>, 2023.~~
- 1550 Stromberg, J. C. and Merritt, D. M.: Riparian plant guilds of ephemeral, intermittent and perennial rivers, *Freshwater Biology*, 61, 1259-1275, 10.1111/fwb.12686, 2016.
- Sweeney, B. W., Bott, T. L., Jackson, J. K., Kaplan, L. A., Newbold, J. D., Standley, L. J., ~~Hession, W. C., and . . .~~ Horwitz, R. J.: Riparian deforestation, stream narrowing, and loss of stream ecosystem services, *Proc. Natl. Acad. Sci. U. S. A.*, 101, 14132-14137, 10.1073/pnas.0405895101, 2004.

- 1555 Tabacchi, E., González, E., Corenblit, D., Garófano-Gómez, V., Planty-Tabacchi, A.-M., and Steiger, J.: Species composition and plant traits: Characterization of the biogeomorphological succession within contrasting river corridors, *River Research and Applications*, 35, 1228-1240, 10.1002/rra.3511, 2019.
- Thoms, M. C. and Parsons, M.: *Eco-geomorphology: an interdisciplinary approach to river science*, International Association of Hydrological Sciences, Publication, 276, 113-119p, 2002.
- 1560 Tomsett, C. and Leyland, J.: Remote sensing of river corridors: A review of current trends and future directions, *River Research and Applications*, 35, 779-803, 10.1002/rra.3479, 2019.
- Tomsett, C. and Leyland, J.: Development and Testing of a UAV Laser Scanner and Multispectral Camera System for Eco-Geomorphic Applications, *Sensors*, 21, 7719, 2021.
- 1565 [UNISDRUnisdr](#) and [CREDCred](#): The Human Cost of Weather Related Disasters: 1995-2015, United Nations Office for Disaster Risk Reduction, 2015.
- Valbuena, R., ~~O'Connor~~^{O'Connor}, B., Zellweger, F., Simonson, W., Vihervaara, P., Maltamo, M., . . . Coops, N. C.: Standardizing Ecosystem Morphological Traits from 3D Information Sources, *Trends in Ecology & Evolution*, 35, 656-667, <https://doi.org/10.1016/j.tree.2020.03.006>, 2020.
- 1570 [vanVan](#) Dijk, W. M., Teske, R., [van-deVan De](#) Lageweg, W. I., and Kleinhans, M. G.: Effects of vegetation distribution on experimental river channel dynamics, *Water Resources Research*, 49, 7558-7574, <https://doi.org/10.1002/2013WR013574>, 2013.
- [vanVan](#) Iersel, W., Straatsma, M., Addink, E., and Middelkoop, H.: Monitoring height and greenness of non-woody floodplain vegetation with UAV time series, *ISPRS Journal of Photogrammetry and Remote Sensing*, 141, 112-123, <https://doi.org/10.1016/j.isprsjprs.2018.04.011>, 2018.
- 1575 [vanVan](#) Leeuwen, B. H.: The consequences of predation in the population biology of the monocarpic species *Cirsium palustre* and *Cirsium vulgare*, *Oecologia*, 58, 178-187, 10.1007/BF00399214, 1983.
- Vasilopoulos, G.: *Characterising the structure and fluvial drag of emergent vegetation*, Geography and the Environment, University of Southampton, 2017.
- 1580 Violle, C., Navas, M. L., Vile, D., Kazakou, E., Fortunel, C., Hummel, I., and Garnier, E.: Let the concept of trait be functional!, *Oikos*, 116, 882-892, 2007.
- Wang, D., Wan, B., Qiu, P., Su, Y., Guo, Q., and Wu, X.: Artificial Mangrove Species Mapping Using Pléiades-1: An Evaluation of Pixel-Based and Object-Based Classifications with Selected Machine Learning Algorithms, *Remote Sensing*, 10, 294, 2018.
- 1585 Whittaker, P., Wilson, C., Aberle, J., Rauch, H. P., and Xavier, P.: A drag force model to incorporate the reconfiguration of full-scale riparian trees under hydrodynamic loading, *Journal of Hydraulic Research*, 51, 569-580, 10.1080/00221686.2013.822936, 2013.
- Wiel, M. J. V. D. and Darby, S. E.: A new model to analyse the impact of woody riparian vegetation on the geotechnical stability of riverbanks, *Earth Surf. Process. Landf.*, 32, 2185-2198, <https://doi.org/10.1002/esp.1522>, 2007.
- 1590 Wilkinson, M. E., Addy, S., Quinn, P. F., and Stutter, M.: Natural flood management: small-scale progress and larger-scale challenges, *Scott. Geogr. J.*, 135, 23-32, 10.1080/14702541.2019.1610571, 2019.

Wilson, C., Bateman, A., Bates, P., and Stoesser, T.: Open Channel Flow through Different Forms of Submerged Flexible Vegetation, *Journal of Hydraulic Engineering*, 129, 10.1061/(ASCE)0733-9429(2003)129:11(847), 2003.

Wilson, C. A. M. E., Yagci, O., Rauch, H. P., and Olsen, N. R. B.: 3D numerical modelling of a willow vegetated river/floodplain system, *Journal of Hydrology*, 327, 13-21, <https://doi.org/10.1016/j.jhydrol.2005.11.027>, 2006.

595 [LiDAR Automatic Unsupervised Segmentation using Segment-Anything Model \(SAM\) from Meta AI: https://github.com/Yarroudh/segment-lidar](https://github.com/Yarroudh/segment-lidar), last

Zhang, Y., Tian, Y., Ding, S., Lv, Y., Samjhana, W., and Fang, S.: Growth, Carbon Storage, and Optimal Rotation in Poplar Plantations: A Case Study on Clone and Planting Spacing Effects, *Forests*, 11, 842, 2020.

1600 Zhao, K., Gong, Z., Zhang, K., Wang, K., Jin, C., Zhou, Z., [Xu, F., and . .](#) Coco, G.: Laboratory Experiments of Bank Collapse: The Role of Bank Height and Near-Bank Water Depth, *Journal of Geophysical Research: Earth Surface*, 125, e2019JF005281, <https://doi.org/10.1029/2019JF005281>, 2020.

Zhao, X., Su, Y., Hu, T., Cao, M., Liu, X., Yang, Q., [Guan, H., Liu, L., and . .](#) Guo, Q.: Analysis of UAV lidar information loss and its influence on the estimation accuracy of structural and functional traits in a meadow steppe, *Ecol. Indic.*, 135, 108515, <https://doi.org/10.1016/j.ecolind.2021.108515>, 2022.

1605 Zhong, L., Cheng, L., Xu, H., Wu, Y., Chen, Y., and Li, M.: Segmentation of Individual Trees From TLS and MLS Data, *IEEE J. Sel. Top. Appl. Earth Observ. Remote Sens.*, 10, 1-14, 10.1109/JSTARS.2016.2565519, 2016.